A THESIS

on

EFFECT OF HEAT TREATMENT ON THE OPTICAL AND STRUCTURAL PROPERTIES OF CdS:Tb NANOFORMS

Submitted in the partial fulfillment of requirement for the award of the Degree of

Master of Science (PHYSICS)

Submitted by: **ANUJA SAXENA**

Roll No.: 30704001

Under the Guidance of

Dr. N.K.VERMA

Professor and Dean

School of Physics and Materials Science

THAPAR UNIVERSITY

PATIALA (PUNJAB)-147 004

JUNE 2009

Dedicated

To

My Parents

CERTIFICATE

This is to certify that the report entitled "**Effect of heat treatment on the optical and structural properties of CdS:Tb nanoforms**" submitted by **Anuja Saxena, Roll No. 30704001**, student of M.Sc (Physics), Thapar University, Patiala, was carried by her under my supervision. She has not submitted this material for credit towards any other degree at Thapar University, Patiala or at any other university.

(N K Verma)
Supervisor
Professor and Dean
School of Physics & Materials Science
Thapar University
Patiala

(O P Pandey)
Professor and Head
School of Physics & Materials Science
Thapar University
Patiala

(R K Sharma) 17/6/09
Dean of Academic Affairs
Thapar University
Patiala

ACKNOWLEDGEMENT

'The real spirit of achieving a goal is through the way of excellence and discipline'

I would have never succeeded in completing my task without the cooperation, encouragement and help provided to me by various personalities. First of all, I render my gratitude to the ALMIGHTY who bestowed self-confidence, ability and strength in me to complete this work.

With deep sense of gratitude I express my sincere thanks to my esteemed and worthy supervisor Dr. N. K. Verma, Professor, School of Physics and Materials Science, for his valuable guidance in carrying out this work under his effective supervision, encouragement, enlightenment and cooperation.

I shall be failing in my duties if I do not express my deep sense of gratitude towards Dr. O. P. Pandey, Professor and Head, School of Physics and Materials Science, who has been a source of inspiration for me throughout this work.

My special thanks to Ms. Zinki Jindal, Mr. Sanjeev Kumar and Mr. Sunil Kumar, Research Scholars, for their timely help, cooperation, useful discussions and good wishes.

I owe my sincere thanks to all the faculty and staff members of School of Physics and Materials Science for their support and encouragement. I would also, like to thank my friends, especially, Manveen Kaur who helped me at various stages during the due course of my work.

My project would not have seen daylight without the immense cooperation and moral support of my parents who kept my spirits up during the endeavor.

Great thanks to all my well wishers.

Anuja Saxena

(ANUJA SAXENA)

Abstract

CdS is an important II-VI semiconductor and has been highlighted as an efficient emitter because of its high quantum yield and direct band gap in the visible range. CdS:Tb nanorods have been synthesized using Solvothermal technique using ethylenediamine as the organic solvent. The samples have been heat treated at 200^{o} C for 2 hours in nitrogen gas atmosphere and the effect on the structural, and optical properties have been studied. The crystal structure and the average crystallite size of the samples have been calculated using X-ray diffraction pattern. The morphology of the nanorods has been studied through SEM images. The elemental analysis has been carried out by EDAX spectroscopy and the FTIR spectroscopy reveals the chemical components on the surface of the nanorods. The band gap of CdS:Tb nanorods, as-synthesized and heat treated, has been calculated by UV-Visible absorption spectra. Room temperature PL studies have been carried out to study the emission characteristics of the synthesized nanoforms.

No structural changes have been observed in XRD patterns. But changes have been observed in morphological and optical characterization with doping and heat treatment.

CONTENTS

Chapter 4: Results and Discussion

Chapter 1

INTRODUCTION

1.1 NANOTECHNOLOGY

1.1.1 History

In the last decade, new directions of modern research have been broadly defined as "nanoscale science and technology [1, 2]. Many nanoforms of matter exist around us. One of the earliest nano-sized objects known to us is made of gold. Faraday prepared colloidal gold in 1856 and called it 'divided metals'.

Figure1.1: Faraday's colloidal gold solution

Metallic gold, when divided into fine particles ranging from sizes of 10-500 nm particles, can be suspended in water. However, the science of nanometer scale objects was not discussed until much later. The cornerstone of nanoscale science, was laid when in 1959, Richard Feynman the Nobel Prize winning physicist entitled "there is plenty of room at the bottom" and envisaged the possibility of arranging atoms to create new matter at the atomic and molecular level.

Feynman described a process by which the ability to manipulate individual atoms and molecules might be developed, using one set of precise tools to build and operate another proportionally smaller set, so on down to the needed scale. In the course of this, he noted

that scaling issues would arise from the changing magnitude of various physical phenomena: gravity would become less important, surface tension and Vander Waals attractions would become more important, etc.

The term "NANOTECHNOLOGY" was coined in 1974 by Norio Taniguchi, professor at Tokyo Science University who pointed out the trend of precision manufacturing at the scale of nanometers. In 1981, Eric Drexler in his MIT doctoral thesis extended the term to a wider area and studied the subject in depth. In the same year, Gerhard Binning and Heinrich Rohrer, who were awarded the Nobel Prize in physics in 1986, invented the Scanning tunneling microscope, a novel measurement tool facilitating the sensing of matter at the nanometer scale. This was a significant technological breakthrough and had a great impact on the future development of 'NANOSCIENCE'. With Nanotechnology being hailed as the science of future and the technology of the next generation, respectively along with their infinite market potential, the key focus lies on the control, manipulation and construction of matter at the atomic and molecular level.

The most prominent area to benefit from nanotechnology is perhaps the electronics industry, which has already achieved remarkable miniaturization by refining the process of photolithography. New structuring techniques have been continuously developed and employed that have led to this miniaturization. As on date, the dimensions of elements that can be fabricated on a semiconductor chip are of the order of one micrometer. Further innovation is required for fabricating materials with nanometer dimensions [3, 4]. Such new methods must also be able to create micro and nanostructures of higher aspect ratios which are often required for microelectronic components [5, 6].

1.1.2 Materials on small scale

Nanotechnology deals with materials or structures in nanometer scale, typically ranging from 1 nm to100 nanometer.

1 nm = 10^{-3} micrometer or 10^{-9} m

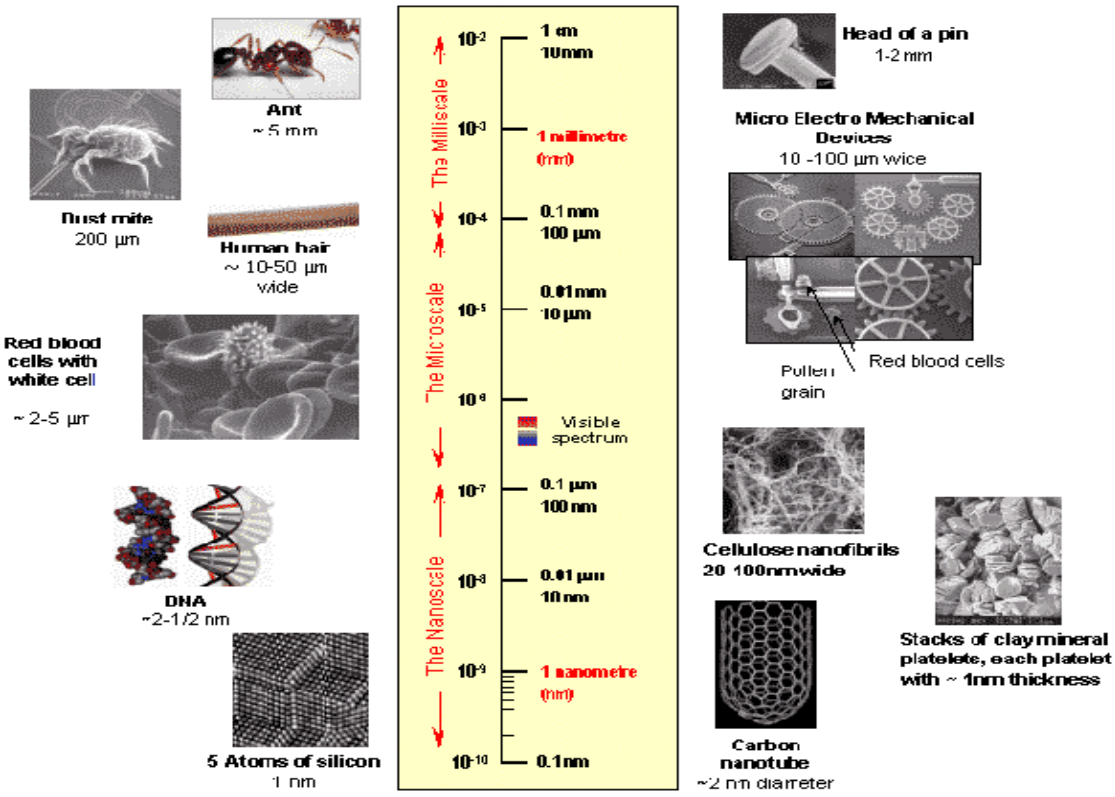

Figure1.2: Illustration of different scales.

Small features permit more functionality in a given space, but nanotechnology is not only a simple continuation of miniaturization from micron meter scale down to nanometer scale. Materials in the micrometer scale mostly exhibit physical properties same as that of bulk form; however, materials in the nanometer scale exhibit physical properties different from that of bulk. Materials in this size range exhibit some remarkable specific properties; a transition from atoms or molecules to bulk form takes place in this size range. For example, crystals in the nanometer scale have a low melting point and reduced lattice constants.

Nanotechnology is design, fabrication and applications of nanostructures or nanomaterials, and the fundamental understanding of the relationships between physical properties or phenomena and material dimensions. With the development of modern understanding of the

materials at nanoscale, we now know that the colors were produced as a result of quantum confinement of electrons in the nanoparticles [7]. In general, nanotechnology refers to the control of matter on the scale of 1 to 100 nanometers, which includes fabrication of matter particles and/or devices within that range.

1.1.3 Effect of nanoscale on properties

The extraordinary aspect at nanoscale is that the physical and chemical properties of a substance may undergo considerable modification because of the following reasons:

1. Increase in surface to volume ratio
2. Quantum confinement

Nanostructures and nanomaterials possess a large fraction of surface atoms per unit volume. The ratio of surface atoms to interior atoms changes dramatically if one successively divides a macroscopic object into smaller parts.

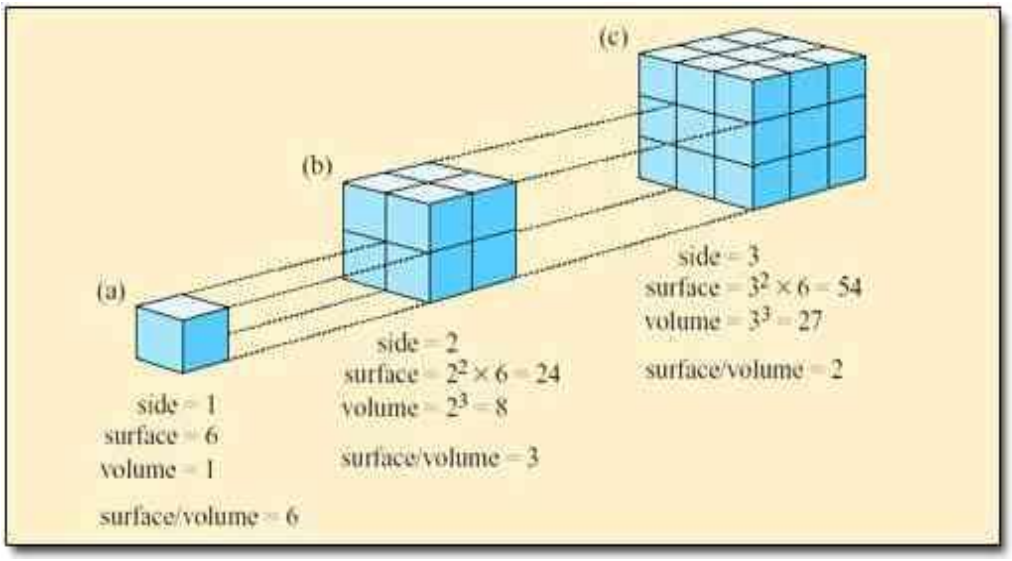

Figure1.3: Example to illustrate increase in Surface to volume ratio

For example, for a cube of 1 cm^3 the percentage of surface atoms would be only 10^{-5} %. When the cube is divided into smaller cubes of an edge of 10 nm, the percentage of surface atoms would increase to 10%. In a cube of 1 nm^3, every atom would be surface atoms [8]. Such a drastic increase in the ratio of surface atoms to interior atoms in nanostructures and nanomaterials might illustrate why changes in size range of nanometers are expected to lead to great changes in physical & chemical properties of the material. The total surface energy increases with the overall surface area, which is in turn strongly dependent on the dimension of material. When the particles change from centimeters size to nanometers size, the surface area and surface energy increase seven orders of magnitude.

Due to the vast surface area, all nanomaterials possess a huge surface energy and thus are thermodynamically unstable or metastable. One of the great challenges in fabrication and processing of nanomaterials is to overcome the surface energy, and to prevent the nanostructures or nanomaterials from growth in size, driven by the reduction of overall surface energy.

Atoms or molecules on a solid surface possess fewer nearest neighbors or coordination numbers, and thus dangling or unsatisfied bonds exposed to the surface. Because of the dangling bonds on the surface, surface atoms or molecules are under an inwardly directed force and the sub-surface atoms or molecules, is smaller than that between interior atoms or molecules. When solid particles are very small, such a decrease in bond length between the surface atoms and interior atoms becomes significant and the lattice constants of the entire solid particles show an appreciable reduction [9].

When atoms form a lattice, the discrete energy levels of the atoms are smudged out into energy bands. The term density of states refers to the number of energy levels in a given interval of energy. In the case of a semiconductor material, the top occupied band, called the valence band, is filled, and there is a small energy separation referred to as the band gap between it and the next higher unfilled conduction band. On the other hand, these bands are overlapping in case of bulk metals, where metal atoms are sort of immersed in a pool of electrons. When a bulk metal particle is reduced in size to a few hundred atoms, dramatic changes occur in the density of states in the conduction band, which is the top band containing electron.

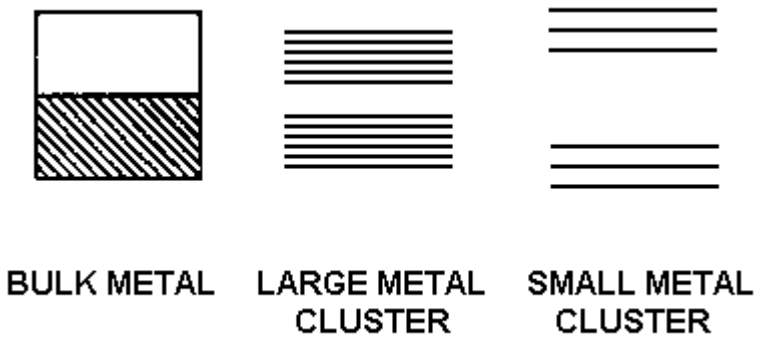

Figure1.4: Changes in energy levels

The continuous density of states in the band is replaced by a set of discrete energy levels, which may have energy level spacing larger than the thermal energy k_BT, so that a gap happens to open up as illustrated in figure 1.4. The changes in the electronic structure during the transition of a bulk metal to a large cluster, and then down to a small cluster of less than 15 atoms [10, 11].The small cluster is analogous to a molecule having discrete energy levels with bonding and anti-bonding orbital. In this situation the energy level can be modeled by the quantum mechanical treatment of the particle in a box. This is referred to as a quantum size effect.

The average energy will not be determined so much by the chemical nature of the atoms, but mainly by the dimension of the particle. It is interesting to note that the quantum size effect occurs in semiconductors at larger sizes because of the longer wavelength of conduction electrons and holes in semiconductors due to the larger effective mass. In a semiconductor the wavelength can approach one micrometer, whereas in metals, it is of the order of 0.5 nm. When the size or dimension of a material is continuously reduced from a large or macroscopic size, such as a meter or a centimeter, to a very small size, the properties remain the same at first, then small changes begin to occur, until finally when the size drops below 100nm, dramatic changes in properties can occur.

If one dimension is reduced to the nano range while the other two dimensions remain large, then we obtain a structure known as a nano well. If two dimensions are reduced and one remains large, the resulting structure is referred to as a nano wire. The extreme case of this process of size reduction in which all three dimensions reach the nanometer range is called a nanoparticle. But if the one, two and three dimensions of nanowell, nanowire and nanoparticle respectively become comparable to Bohr exciton radius, then these structures are known as quantum well, quantum wire and quantum dot respectively. Confinement in these structures is known as quantum confinement.

An ‘exciton’ is the term used to describe the electron-hole pair created when an electron leaves the valence band and enters the conduction band as shown in the figure 1.5. An exciton is a quantum of electronic excitation energy travelling in the periodic structure of a crystal; it is electrically neutral and hence its movement through the crystal gives rise to the transportation of energy but not charge. Excitons have a natural physical separation between the electron and the hole that varies from substance to substance; this average distance is called the Exciton Bohr Radius. A vivid picture of exciton formation is as follows: a photon enters a semiconductor, exciting an electron from the valence band into the conduction band. The missing electron in the valence band leaves a hole (of opposite electric charge) behind, to which the electron is attracted by the Coulomb force. The exciton results from the binding of the electron with its hole. As a result, the exciton has slightly less energy than the unbound electron and hole. The wavefunction of the bound state is hydrogenic (an exotic atom state akin to that of a hydrogen atom). However, the binding energy is much smaller and the size much bigger than a hydrogen atom because of the effective mass of the constituents in the material. In a large semiconductor crystal, the Exciton Bohr Radius is small compared to the crystal, and the exciton is free to wander throughout the crystal.

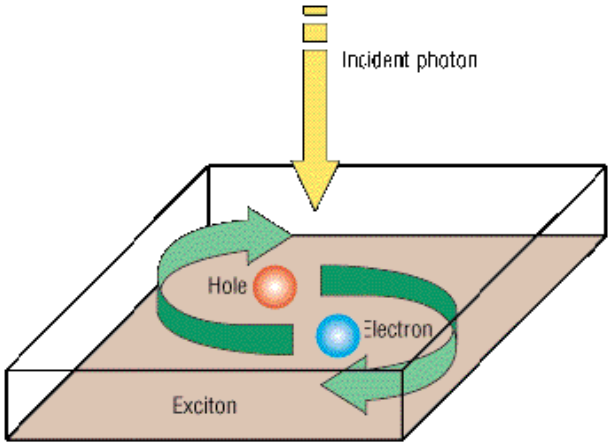

Figure1.5: Schematic view of how an exciton is formed.

In a quantum dot, the Exciton Bohr Radius is on the order of the physical dimension of the dot or smaller, and the exciton is confined. This second set of conditions is called quantum confinement, which is synonymous with having discrete, rather than continuous energy levels. The size of this radius controls how large a crystal must be before its energy bands can be treated as continuous. Therefore, the Exciton Bohr Radius can rightly be said to define whether a crystal can be called a semiconductor quantum dot, or simply a bulk semiconductor.

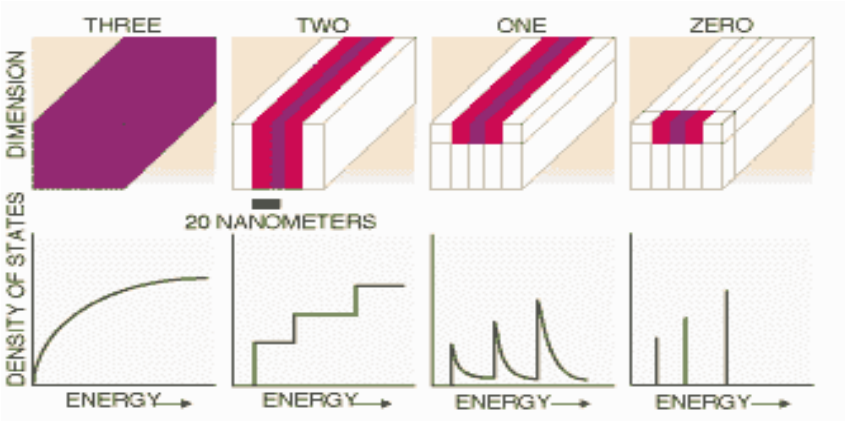

Figure1.6: Quantum confinement in 0-D, 1-D, 2-D and 3-D

The word quantum is associated with these three types of nanostructures, as shown in figure 1.6, because the changes in properties arise from the quantum-mechanical nature of physics in the domain of the ultrasmall.

For one thing, it leads to new electronic properties that are not present in today's semiconductor devices. A quantum dot exhibits 0-D confinement, meaning that electrons are confined in all three dimensions. The only things in nature that have 0-D confinement are atoms. So a quantum dot can be loosely described as an 'artificial atom'. This is vitally important because we can't readily experiment on regular atoms. They're too small and too difficult to isolate in an experiment. Quantum dots, on the other hand, are large enough to be manipulated by magnetic fields and can even be moved around with an STM or AFM. We can deduce many important atomistic characteristics from a quantum dot that would otherwise be impossible to research in an atom.

Confinement also increases the efficiency of today's electronics. The laser is based on a 2-D confinement layer that is usually created with some form of Chemical Vapor Deposition. The bulk of modern lasers created with this method are highly functional, but ultimately inefficient in terms of energy consumption and heat dissipation. Moving to 1-D confinement in wires or 0-D confinement in quantum dots allows for higher efficiencies and brighter lasers. Quantum dot lasers are currently the best lasers available though their fabrication is still being worked out. Quantum confinement describes the increase in energy which occurs when the motion of a particle is restricted in one or more dimensions by a potential well. When the confining dimension is large compared to the wavelength of the particle, the particle behaves as if it were free. As the confining dimension decreases, the particle's energy increases.

1.2 Fabrication Techniques

There are two approaches for the synthesis of nanomaterials:

- **Top-down**
- **Bottom-up**

There are various top-down and bottom-up approaches when fabricating metal nano/microwires including various lithographic techniques [12, 13], self-assembly [14] and direct evaporation through a shadow mask [15]. Attrition or milling is a typical top-down method in making nanoparticles, whereas the colloidal dispersion is a good example of bottom-up approach in the synthesis of nanoparticles. Lithography may be considered as a hybrid approach, since the growth of thin films is bottom-up whereas etching is top-down, while nanolithography and nano manipulations are commonly a bottom-up approach. Both approaches play very important roles in modern industry and most likely in nanotechnology as well. There are advantages and disadvantages in both approaches.

Among others, the biggest problem with top-down approach is the imperfection of the surface structure. It is well known that the conventional top-down techniques can cause significant crystallographic damage to the processed patterns [16], and additional defects may be introduced even during the etching steps [17]. For example, nanowires made by lithography are not smooth and may contain lot of impurities and structural defects on surface. Such imperfections would have a significant impact on physical properties and surface chemistry of nanostructures and nanomaterials, since the surface over volume ratio in nanostructures and nanomaterials is very large.

Bottom-up approach refers to the build-up of a material from the bottom: atom-by-atom, molecule-by-molecule, or cluster-by-cluster. In crystal growth, growth, growth species, such as atoms, ions and molecules, after impinging onto the growth surface, assemble into crystal structure one after another. Although the bottom-up approach is nothing new, it plays an important role in the fabrication and processing of nanostructures and nanomaterials. There are several reasons for this. When structures fall into a nanometer scale, there is little choice for top-down approach. All the tools we have possessed are too big to deal with such tiny subjects.

Bottom-up approach also promises a better chance to obtain nanostructres with less defects, more homogeneous chemical composition, and better short and long range ordering. This is because the bottom-up approach is driven mainly by the reduction of Gibbs free energy, so that nanostructures and nanomaterials such produced are in a state closer to a thermodynamic equilibrium state. On the

contrary, top-down approach most likely introduces internal stress, in addition to surface defects and contaminations.

1.3 APPLICATIONS

Nanotechnology offers an extremely broad range of potential applications from electronics, optical communications and biological systems to new materials. Many possible applications have been explored and many devices and systems have been studied. More potential applications and new devices are being proposed in literature. It is obviously impossible to summarize all the devices and applications that have been studied and it is impossible to predict new applications and devices. It is interesting to note that the applications of nanotechnology in different fields have distinctly different demands, and thus face very different challenges, which require different approaches. For example, for applications in medicine, or in nanomedicine, the major challenge is "miniaturization": new instruments to analyze tissues literally down to the molecular level, sensors smaller than a cell allowing looking at ongoing functions, and small machines that literally circulate within a human body pursuing pathogens and neutralizing chemical toxins [18, 19].

Applications of nanostructured and nanomaterials are based on:

(i) the peculiar physical properties of nanosized materials, e.g. gold nanoparticles used as inorganic dye to introduce colors into glass and as low temperature catalyst,

(ii) the huge surface area, such as mesoporous titania for photo-electrochemical cells, and nanoparticles for various sensors, and

(iii) small size that offers extra possibilities for manipulation and room for accommodating multiple functionalities.

For many applications, new materials and new properties are introduced. For example, various organic molecules are incorporated into electronic device, such as sensors [19].

1.3.1 Molecular Electronics and Nanoelectronics

Tremendous efforts and progress have been made in the molecular electronics and nanoelectronics [20, 21]. In molecular electronics, single molecules are expected to be able to control electron transport, which offers the promise of exploring the vast variety of molecular functions for electronics devices, and molecules can now be crafted into a working circuit.

Current high-technology production processes are based on traditional top down strategies, where nanotechnology has already been introduced silently. The critical length scale of integrated circuits is already at the nanoscale (50 nm and below) regarding the gate length of transistors in CPUs or DRAM devices.

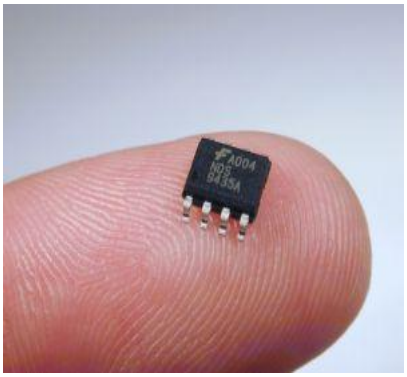

Figure1.7: View of a nano-chip

Electronic memory designs in the past have largely relied on the formation of transistors however research into crossbar switch based electronics have offered an alternative using reconfigurable interconnections between vertical and horizontal wiring arrays to create ultra high density memories..

1.3.2 Medicine

The biological and medical research communities have exploited the unique properties of nanomaterials for various applications (e.g., contrast agents for cell imaging and therapeutics for treating cancer). Terms such as biomedical nanotechnology, bio-nanotechnology, and

nanomedicine are used to describe this hybrid field. Functionalities can be added to nanomaterials by interfacing them with biological molecules or structures. The size of nanomaterials is similar to that of most biological molecules and structures; therefore, nanomaterials can be useful for both in vivo and in vitro biomedical research and applications. Thus far, the integration of nanomaterials with biology has led to the development of diagnostic devices, contrast agents, analytical tools, physical therapy applications, and drug delivery vehicles.

Figure 1.8: Nano drugs

Magnetic nanoparticles, bound to a suitable antibody, are used to label specific molecules, structures or microorganisms. Gold nanoparticles tagged with short segments of DNA can be used for detection of genetic sequence in a sample. Multicolor optical coding for biological assays has been achieved by embedding different-sized quantum dots into polymeric microbeads. Nanopore technology for analysis of nucleic acids converts strings of nucleotides directly into electronic signatures. Another vision is based on small electromechanical systems; NEMS are being investigated for the active release of drugs. Some potentially important applications include cancer treatment with iron nanoparticles or gold shells.

1.3.3 Heavy Industry

An inevitable use of nanotechnology will be in heavy industry. Lighter and stronger materials will be of immense use to aircraft manufacturers, leading to increased performance. Spacecraft will also be benefited, where weight is a major factor. Nanotechnology would help to reduce the size of equipment and thereby decrease fuel-consumption required to get it airborne.

Hang gliders halve their weight while increasing their strength and toughness through the use of nanotech materials. Nanotech is lowering the mass of super capacitors that will increasingly be used to give power to assistive electrical motors for launching hang gliders off flatland to thermal-chasing altitudes.

Nanotechnology has the potential to make construction faster, cheaper, safer, and more varied. Automation of nanotechnology construction can allow for the creation of structures from advanced homes to massive skyscrapers much more quickly and at much lower cost.

Using nanotech applications, refineries producing materials such as steel and aluminum will be able to remove any impurities in the materials they create. Much like aerospace, lighter and stronger materials will be useful for creating vehicles that are both faster and safer. Combustion engines will also benefit from parts that are more hard-wearing and more heat-resistant.

1.3.4 Nanomechanics

Nanomechanics is a branch of *nanoscience* studying fundamental *mechanical* (elastic, thermal and kinetic) properties of physical systems at the nanometer scale. Nanomechanics has emerged on the cross-road of classical mechanics, solid-state physics, statistical mechanics, materials science, and quantum chemistry. As an area of nanoscience, nanomechanics provide a scientific foundation of nanotechnology.

Often, nanomechanics is viewed as a *branch* of nanotechnology, i.e., an applied area with a focus on the mechanical properties of *engineered* nanostructures and nanosystems (systems with nanoscale components of importance). Examples of the latter include nanoparticles, nanopowders, nanowires, nanorods, nanoribbons, nanotubes, including carbon nanotubes (CNT)

and boron nitride nanotubes (BNNTs); nanoshells, nanomebranes, nanocoatings, nanocomposite/nanostructured materials, nanofluids (fluids with dispersed nanoparticles); nanomotors, etc. Some of the well-established *fields of nanomechanics* are: nanomaterials, nanotribology (friction, wear and contact mechanics at the nanoscale), nano electromechanical systems (NEMS), and nanofluidics.

Apart from these there are many more applications which are being or will be explored in this field.

1.4. Literature Review

Chalcogenide nanomaterials have been attracting a lot of attention from the researchers all over the world due to their physical and chemical properties: Photoluminescence being the property of immense interest. There is a lot of literature available on the photoluminescence and structural properties of CdS nanoparticles.

Luminescence is the process, where an electromagnetic radiation is produced by a substance under suitable external excitation. At certain frequencies, this radiation is significantly in excess of the thermal radiation, which is emitted by a substance at that particular temperature. The so-produced electromagnetic radiation, generally in the visible region, is characteristic of the particular luminescent material under examination, termed as phosphor [22]. CdS is a direct band II-VI semiconductor, with a band gap of 2.4eV. CdS has vital optoelectronic applications for laser light-emitting diodes and optical devices based on nonlinear properties [23]. To alter the properties of chalcogenides in a positive way, these are doped with various materials. Doping of CdS nanorods is done to improve their photoluminescent properties. To enhance the luminescent properties of the chalcogenides they have been doped with rare earth metals, i.e., Europium, Terbium, Yttrium etc. Rare earth ions are used as the active ions in luminescent materials used in optoelectronics applications, most notably the Nd:YAG laser. Phosphors with rare earth dopants are also widely used in cathode ray tube technology such as television sets. The earliest color television CRTs had a poor-quality red; europium as a phosphor dopant made good red phosphors possible. The rare earth doped nanocrystalline phosphors have been used for field emission displays [24-26]. Tiseanu et al. [27] have studied the optical properties of terbium

doped thiosalicylic-capped CdS nanocrystals and comparative study of time-resolved photoluminescence properties of terbium-doped thiosalicylic-capped CdS and ZnS nanocrystals. Jyothy et al. [28] has studied fluorescence enhancement in Tb^{3+}/CdS nanoparticles doped silica xerogels. Hua et al. [29] has studied the doping of terbium in ZnS. They have shown electroluminescent properties of a device based on terbium-doped ZnS nanocrystals. [30] Co-doping of CdS nanoparticles using Li^{+}, Eu^{3+} has been done. Eu^{3+} doped CdS [31] nanocrystals, via, sol-gel method has been found in the literature.

In our present study, we have synthesized and studied various properties of CdS nanorods, doped with Terbium, by varying the concentration of Terbium, which has been discussed in chapter 3, and then by providing heat treatment to the samples at 200^{0} C for 2 hours in nitrogen gas atmosphere.

Chapter 2

MATERIALS AND CHARACTERIZATION

2.1 Semiconductor Nanoparticles

The electronic and optical properties of II-VI compound semiconductor nanoparticles have been extensively investigated in view of a wide variety of applications [32]. With change in the particle size, dramatic modifications of their electronic and optical properties takes place due to the three-dimensional quantum confinement of electrons and holes when the size of the particle approaches the Bohr radius of an exciton [33, 34]. In addition to the change in electronic and optical properties, the structural behavior also exhibits changes with change in particle size. It is well known that bulk CdS has a stable wurtzite (hexagonal) structure from room temperature to melting point. However, metastable cubic phase has been found in thin films and nanocrystalline powders [35, 36].

Semiconductors with widely tunable energy band gap are considered to be the materials for next generation flat panel displays, photovoltaic, optoelectronic devices, laser, sensors, photonic band gap devices, etc.

2.2 Cadmium sulphide

Cadmium sulphide is a chemical compound with the formula CdS. Cadmium sulphide is yellow in color and is a semiconductor [37]. It exists in nature as two different minerals, greenockite [37] and hawleyite [38]. It is a direct band gap semiconductor (2.42 eV) [39] and has many applications for example in light detectors. Cadmium sulphide has, like zinc sulphide, two crystal forms; the more stable hexagonal wurtzite structure (found in the mineral Greenockite) and the cubic zinc blende structure (found in the mineral Hawleyite)[40].

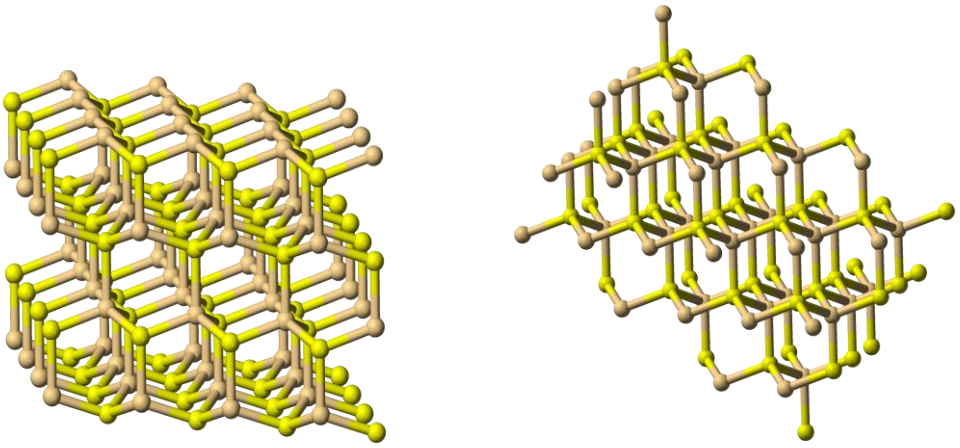

(a) **(b)**

Figure 2.1: (a) Greenockite (wurtzite) ,(b) Hawleyite (cubic structure)

Some of the application based properties of CdS are as follows:

- When irradiated with light, the conductivity of CdS increases [39] (used as a photoresistor)
- When combined with a p-type semiconductor it forms the core component of a photovoltaic (solar) cell. Moreover, CdS/Cu_2S solar cell was one of the first efficient cells to be reported (1954) [41, 42].
- When fabricated in thin films, it can form transistors [43, 44].
- When doped with Cu^+ ("activator") and Al^{3+} ("coactivator"), CdS shows luminescence under electron beam excitation (cathodoluminescence) and is used as phosphor [45].
- Both polymorphs are piezoelectric and the hexagonal form is pyroelectric [46, 47] and electroluminescent[48].
- CdS crystal can act as a solid state laser [49, 50]

2.3 Terbium

Terbium is a soft, malleable, ductile, silver-gray metal member of the lanthanide group of the periodic table. It is reasonably stable in air, but it is slowly oxidized [51] and it reacts with cold water. Terbium is one of the rarer rare-earth elements, although is twice as common in the Earth's crust as silver. It is reasonably stable in air, and two crystal allotropes exist, with a transformation temperature of 1289 °C [52]. It is never found in nature as free element, but is contained in many minerals. The most important ores are monazite, bastnasite and cerite.

The Terbium(III) cation is brilliantly fluorescent, in a bright lemon-yellow color that is the result of a strong green emission line in combination with other lines in the orange and red. The yttrofluorite variety of the mineral fluorite owes its creamy-yellow fluorescence in part to terbium.

The physical properties of terbium are listed below:

Phase	solid
Density Liquid density at M.P.	8.23 $g \cdot cm^{-3}$ 7.65 $g \cdot cm^{-3}$
Melting point	1629K (1356°C, 2473°F)
Boiling point	3503 K (3230°C, 5846°F)
Heat of fusion	10.15 $kJ \cdot mol^{-1}$
Heat of vaporization	293 $kJ \cdot mol^{-1}$
Specific heat capacity	(25°C) 28.91 $J \cdot mol^{-1} \cdot K^{-1}$

2.4 Effect of Doping

II-VI semiconductor nanocrystals have been extensively investigated during the past decades. Their unique optical properties due to quantum confinement effects are always of interest for the possible application in optoelectronics. Doped nanocrystals are worth of investigating in more details because band gap of nanocrystalline hosts can be adjusted by sizes to match the energy levels of luminescent centers and thus new luminescence is expected.

It is well known that rare earth (RE) elements are effective luminescent centres [53, 54]. RE-doped luminescent II-VI materials, for example, Tb, Eu, Ce and Sm doped CaS and SrS, are promising candidates for application in color thin-film electroluminescence devices [55]. But the instability and hygroscopic nature of CaS and SrS are problems in their application. As we know CdS is more stable than Cas or SrS as host of luminescent materials. But in Tb-doped CdS crystals the characteristic emission due to *f-d* transition in Tb^{3+} centers cannot be observed for the reason that band gap of CdS semiconductor host is not so wide as alkaline earth sulfides.

Doping a semiconductor crystal introduces allowed energy states within the band gap but very close to the energy band that corresponds to the dopant type. In other words, donor impurities create states near the conduction band while acceptors create states near the valence band. The gap between these energy states and the nearest energy band is usually referred to as dopant-site bonding energy and it is relatively small. Dopants also have the important effect of shifting the material's Fermi level towards the energy band that corresponds with the dopant with the greatest concentration. Since the Fermi level must remain constant in a system in thermodynamic equilibrium, stacking layers of materials with different properties leads to many useful electrical properties.

2.5 CHARACTERIZATION TECHNIQUES

Characterization of nanomaterials and nanostructures has been largely based on the surface analysis techniques and conventional characterization methods developed for bulk materials. The morphological features have been studied through Scanning Electron Microscopy (SEM), while their crystal structure has been investigated through X-ray diffraction (XRD) studies. Fourier transform infrared spectroscopy (FTIR) and Energy

dispersion X-ray spectroscopy (EDX) has also been used to study the chemical composition of the sample. The optical studies have been carried out using UV-visible absorption and Photoluminescence (PL) studies.

2.5.1 X-Ray Diffraction

X-ray powder diffraction (XRD) is a rapid analytical technique primarily used for phase identification of crystalline material and can provide information on unit cell dimensions. It is a versatile, non-destructive technique that reveals detailed information about the chemical composition and crystallographic structure of natural and manufactured materials.

By varying the angle theta, the Bragg's Law conditions are satisfied by different d-spacing in polycrystalline materials.

$$n\lambda = 2d\sin\theta \qquad \text{…. (2.1)}$$

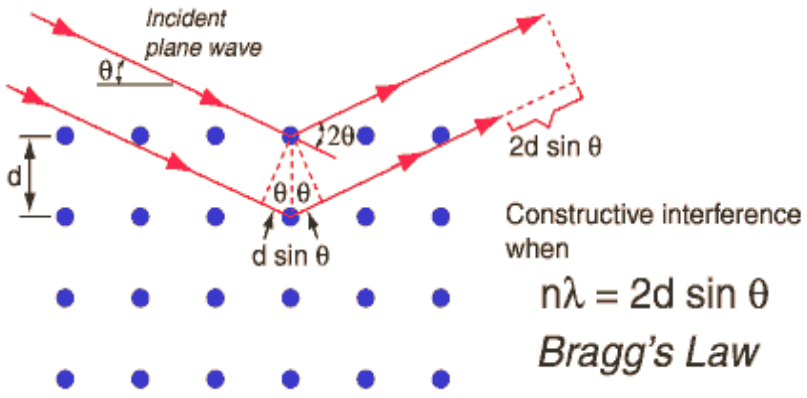

Figure 2.2: Schematic for Bragg's Law

Max von Laue, in 1912, discovered that crystalline substances act as three-dimensional diffraction gratings for X-ray wavelengths similar to the spacing of planes in a crystal lattice. X-ray diffraction is now a common technique for the study of crystal structures and atomic spacing.

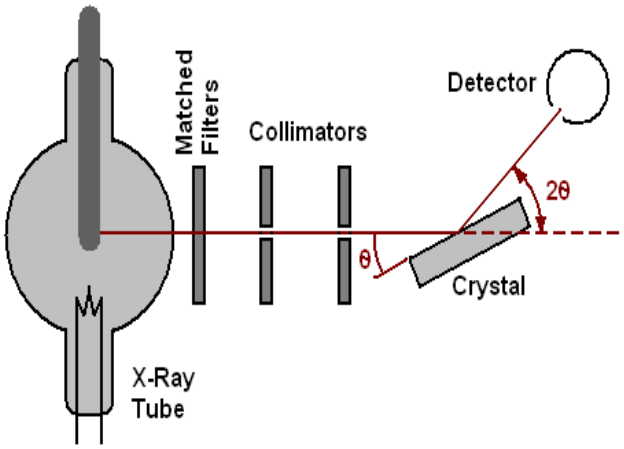

Figure2.3: Schematic for X-Ray diffraction

X-ray diffraction is based on constructive interference of monochromatic X-rays and a crystalline sample. These X-rays are generated by a cathode ray tube, filtered to produce monochromatic radiation, collimated to concentrate, and directed toward the sample. The interaction of the incident rays with the sample produces constructive interference (and a diffracted ray) when conditions satisfy Bragg's Law. This law relates the wavelength of electromagnetic radiation to the diffraction angle and the lattice spacing in a crystalline sample. These diffracted X-rays are then detected, processed and counted. A detector records and processes this X-ray signal and converts the signal to a count rate which is then output to a device such as a printer or computer monitor.

The geometry of X-ray diffractometer is such that the sample rotates in the path of the collimated X-ray beam at an angle θ while the X-ray detector is mounted on an arm to collect the diffracted X-rays and rotates at an angle of 2θ. The instrument used to maintain the angle and rotate the sample is termed a goniometer. By scanning the sample through a range of 2θ angles, all possible diffraction directions of the lattice should be attained due to the random orientation of the powdered material. Conversion of the diffraction peaks to d-spacing allows identification of the mineral because each mineral

has a set of unique d-spacing. Typically, this is achieved by comparison of d-spacing with standard reference patterns.

All diffraction methods are based on generation of X-rays in an X-ray tube. These X-rays are directed at the sample, and the diffracted rays are collected. A key component of all diffraction is the angle between the incident and diffracted rays. For typical powder patterns, data is collected at 2θ from ~5° to 70°, angles that are preset in the X-ray scan.

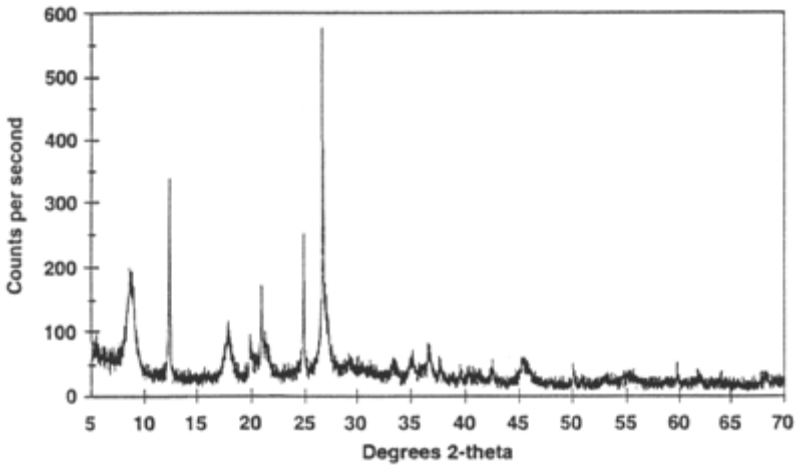

Figure 2.4: Diffraction peaks of a sample.

2.5.2 Energy Dispersion X-Ray Spectroscopy (EDX)

Energy dispersive X-ray spectroscopy (EDS, EDX or EDXRF) is an analytical technique used for the elemental analysis or chemical characterization of a sample. As a type of spectroscopy, it relies on the investigation of a sample through interactions between electromagnetic radiation and matter, analyzing X-rays emitted by the matter in response to being hit with charged particles. Its characterization capabilities are due in large part to the fundamental principle that each element has a unique atomic structure allowing X-rays that are characteristic of an element's atomic structure to be

identified uniquely from each other rays that are characteristic of an element's atomic structure to be identified uniquely from each other.

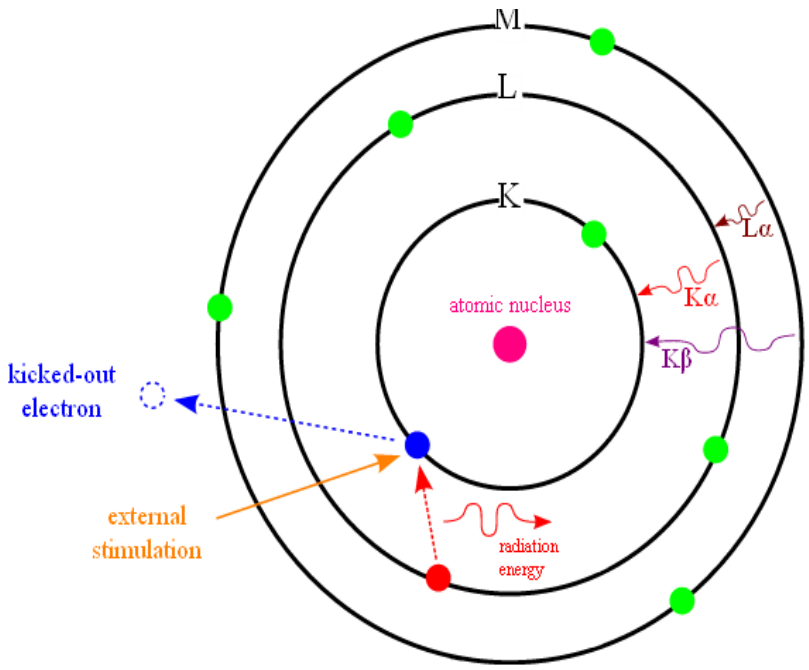

Figure 2.5: Illustration of the principle of EDX

To stimulate the emission of characteristic X-rays from a specimen, a high energy beam of charged particles such as electrons or protons, or a beam of X-rays, is focused into the sample being studied. At rest, an atom within the sample contains ground state (or unexcited) electrons in discrete energy levels or electron shells bound to the nucleus. The incident beam may excite an electron in an inner shell, ejecting it from the shell while creating an electron hole where the electron was. An electron from an outer, higher-energy shell then fills the hole, and the difference in energy between the higher-energy shell and the lower energy shell may be released in the form of an X-ray. The number and energy of the X-rays emitted from a specimen can be measured by an energy dispersive spectrometer. As the energy of the X-rays is characteristic of the difference in energy

between the two shells, and of the atomic structure of the element from which they were emitted, this allows the elemental composition of the specimen to be measured.

The energy of the X-ray photon depends on the element of which the electron was a part, as well as the initial and final states of the electron making the transition. These energies are predictable. X-ray producing transitions are commonly grouped into categories based on the initial and final states of the electron. These transitions are labeled as X_J, with X denoting the final state shell of the electron (K for n = 1, L for n = 2, M for n = 3, and so on), and J indicating how many shells above the final state the electron transitioned from (i = α, β, γ, … for 1, 2, 3, … respectively). For example, $L_ß$ would indicate that the electron transitioned to the n = 2 shell, from 2 shells above (n = 4).

Typically K_α (K-alpha) X-ray transitions are the strongest emission lines seen, which occur when an electron transitions from the *n = 2* shell to the *n = 1* shell. The energy given off (in the form of an X-ray photon) can calculated as,

$$E_{K_\alpha} = E_0 \, (Z-1)^2 \left(\frac{1}{1^2} - \frac{1}{2^2}\right) \qquad \textbf{(2.2)}$$

Where $E_0 = 13.6\ eV$, and Z (an integer ≥ 2) is the atomic number of the atom This simplifies to,

$$E_{K_\alpha} = (10.2\ \text{eV})\,(Z-1)^2 \qquad \textbf{(2.3)}$$

Further refinements can be made by taking into account more of the quantum numbers describing the states from which the electrons transition to / from, such as the angular momentum and spin, as well as selection rules describing which transitions are allowed.

2.5.3 Scanning electron microscopy (SEM)

The scanning electron microscope (SEM) is a type of electron microscope that images the sample surface by scanning it with a high-energy beam of electrons in a raster scan pattern. The SEM is a microscope that uses electrons instead of light to form an image. The electrons interact with the atoms that make up the sample producing signals that contain information about the sample's surface topography, composition and other properties such as electrical conductivity. The scanning electron microscope has many advantages over traditional microscopes. The SEM has a large depth of field, which allows more of a specimen to be in focus at one time. The SEM also has much higher resolution (~ 1 nm), so closely spaced specimens can be magnified at much higher levels. Because the SEM uses electromagnets rather than lenses, the researcher has much more control in the degree of magnification. All of these advantages, as well as the actual strikingly clear images, make the scanning electron microscope one of the most useful instruments in research today.

In a typical SEM, an electron beam is thermionically emitted from an electron gun fitted with a tungsten filament cathode. Tungsten is normally used in thermionic electron guns because it has the highest melting point and lowest vapor pressure of all metals. The electron beam, which typically has an energy ranging from a few hundred eV to 40 keV, is produced at the top of the microscope by an electron gun. The electron beam follows a vertical path through the microscope, which is held within a vacuum. The beam passes through pairs of scanning coils or pairs of deflector plates in the electron column, typically in the final lens, which deflect the beam in the *x* and *y* axes so that it scans in a raster fashion over a rectangular area of the sample surface.Once the beam hits the sample, electrons and X-rays are ejected from the sample.

Detectors collect these X-rays, backscattered electrons, and secondary electrons and convert them into a signal that is sent to a screen similar to a television screen. This produces the final image.

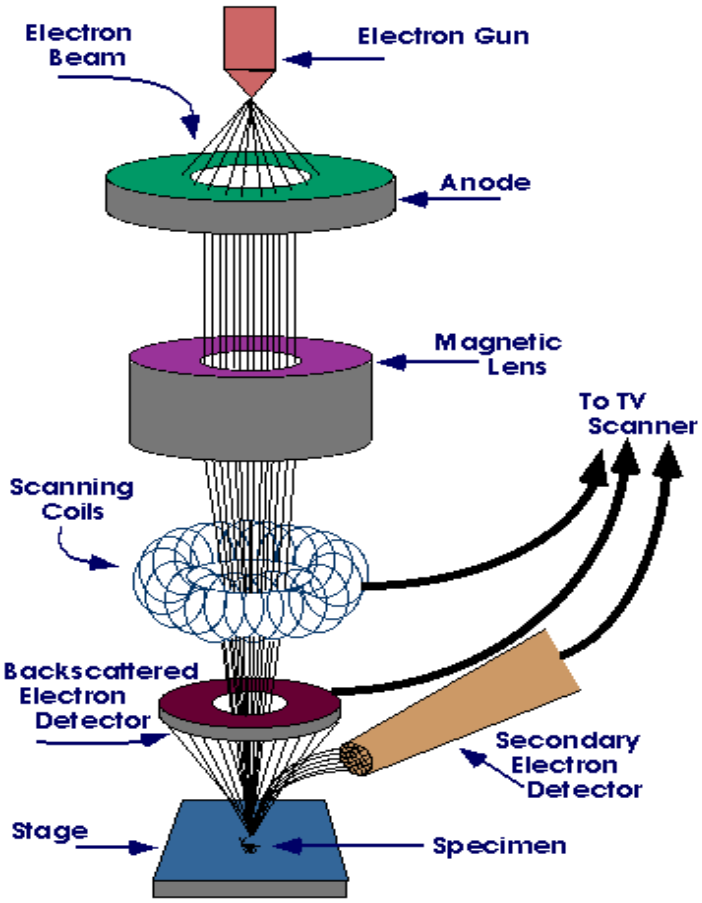

Figure 2.6: Schematic diagram of a scanning electron microscope.

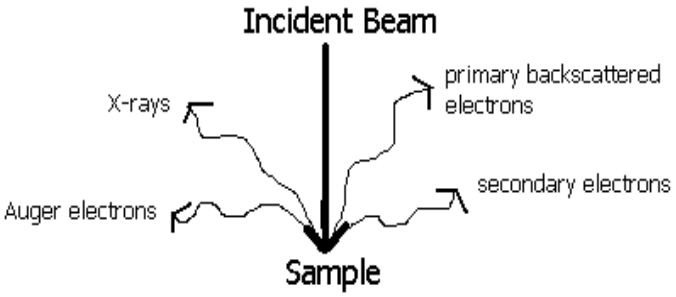

Figure 2.7: Signals produced by an electron beam incident on the specimen.

All samples must also be of an appropriate size to fit in the specimen chamber and are generally mounted rigidly on a specimen holder called a specimen stub. Several models of SEM can examine any part of a 6-inch (15 cm) semiconductor wafer, and some can tilt an object of that size to 45 degrees.

For conventional imaging in the SEM, specimens must be electrically conductive, at least at the surface, and electrically grounded to prevent the accumulation of electrostatic charge at the surface. Metal objects require little special preparation for SEM except for cleaning and mounting on a specimen stub. Nonconductive specimens tend to charge when scanned by the electron beam, and especially in secondary electron imaging mode, this causes scanning faults and other image artifacts. They are therefore usually coated with an ultra thin coating of electrically-conducting material, commonly gold, deposited on the sample either by low vacuum sputter coating or by high vacuum evaporation. Conductive materials in current use for specimen coating include gold, gold/palladium alloy, platinum, osmium, iridium, tungsten, chromium and graphite. Coating prevents the accumulation of static electric charge on the specimen during electron irradiation.

Two important reasons for coating, even when there is more than enough specimen conductivity to prevent charging, are to maximize signal and improve spatial resolution, especially with samples of low atomic number (Z). Broadly, signal increases with atomic number, especially for backscattered electron imaging. The improvement in resolution arises because in low-Z materials such as carbon, the electron beam can penetrate several micrometers below the surface, generating signals from an interaction volume much larger than the beam diameter and reducing spatial resolution. Coating with a high-Z material such as gold maximizes secondary electron yield from within a surface layer a few nm thick, and suppresses secondary electrons generated at greater depths, so that the signal is predominantly derived from locations closer to the beam and closer to the specimen surface than would be the case in an uncoated, low-Z material.

2.5.4 Fourier Transform Infra-red Spectroscopy (FTIR)

FTIR is most useful for identifying chemicals that are either organic or inorganic. It can be utilized to quantitate some components of an unknown mixture. It can be applied to the analysis of solids, liquids, and gasses. The term Fourier Transform Infrared Spectroscopy (FTIR) refers to a fairly recent development in the manner in which the data is collected and converted from an interference pattern to a spectrum. FTIR is perhaps the most powerful tool for identifying types of chemical bonds (functional groups). The wavelength of light absorbed is characteristic of the chemical bond as can be seen in the spectrum. By interpreting the infrared absorption spectrum, the chemical bonds in a molecule can be determined.

Molecular bonds vibrate at various frequencies depending on the elements and the type of bonds. For any given bond, there are several specific frequencies at which it can vibrate. According to quantum mechanics, these frequencies correspond to the ground state (lowest frequency) and several excited states (higher frequencies). One way to cause the frequency of a molecular vibration to increase is to excite the bond by having it absorb light energy. For any given transition between two states the light energy (determined by the wavelength) must exactly equal the difference in the energy between the two states [*usually ground state (E_0) and the first excited state (E_1)]*.

The energy corresponding to these transitions between molecular vibrational states is generally 1-10 kilocalories/mole which corresponds to the infrared portion of the electromagnetic spectrum.

Difference in energy = Energy of light Absorbed

$$E_1 - E_0 = h\,c / l \qquad (2.4)$$

Where h = *Plank's constant*

c = *speed of light*

An interferometer utilizes a beamsplitter to split the incoming infrared beam into two optical beams. One beam reflects off of a flat mirror which is fixed in place. Another beam reflects off of a flat mirror which travels a very short distance (typically a few millimeters) away from the beamsplitter. The two beams reflect off of their respective mirrors and are recombined when they meet together at the beamsplitter.

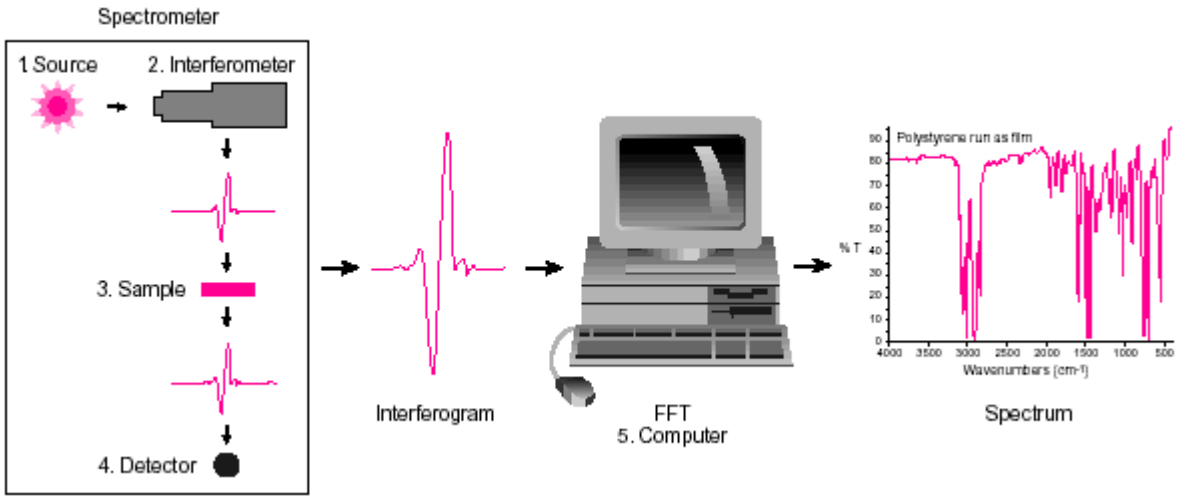

Figure 2.8: Basic components of FTIR

Because the path that one beam travels is a fixed length and the other is constantly changing as its mirror moves, the signal which exits in the interferometer is the result of these two beams "interfering" with each other. Consequently, the resulting signal is called interferogram, which has every infrared frequency encoded into it.

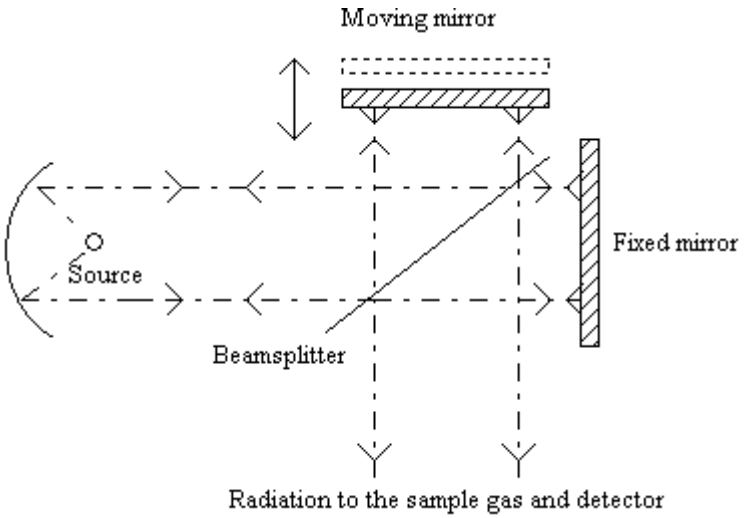

Figure 2.9: Illustration of working of an interferometer in FTIR

When the interferogram signal is transmitted through or reflected off of the sample surface, the specific frequencies of energy are adsorbed by the sample due to the excited vibration of function groups in molecules. The infrared signal after interaction with the sample is uniquely characteristic of the sample.

The beam finally arrives at the detector and is measured by the detector. The detected interferogram can not be directly interpreted. It has to be "decoded" with Fourier Transformation. The computer can perform the Fourier transformation calculation and present an infrared spectrum, which plots absorbance (or transmittance) versus wavenumber.

2.6 OPTICAL CHARACTERIZATION

Optical spectroscopy has been widely used for the characterization of nanomaterials, and it can be categorized into two groups: absorption and emission spectroscopy. The absorption and emission spectroscopy determines the electronic structures of atoms, ions, molecules or crystals through exciting electrons from the ground to excited states (absorption) and relaxing from excited to ground states (emission). In this section, UV-

Visible spectroscopy and photoluminescence has been used to determine the optical properties of the samples.

2.6.1 UV-Visible spectroscopy

UV-Vis absorption spectroscopy is the measurement of the attenuation of the beam of light after it passes through a sample or after reflection from a sample surface. UV-Vis includes transmittance, absorption and reflection measurements in UV, VISIBLE and Near Infra Red region.

Light Range: 190-900 nm

Lower wavelength limit exists because of the absorption of <180 nm by atmospheric gases. We can get a limit of 175 nm if we purge the spectrometer with nitrogen gas. For working to <175 nm we need a vacuum spectrometer. The upper wavelength limit is determined by the wavelength response of the detector in the spectrometer.

2.6.1.1 Information:

- Quantative measurement of an analyte.
- Optical and electronic properties of the materials: UV and visible photons can promote electrons to higher energy states in the molecules and materials.

2.6.1.2 Principle:

"Beer-Lambert's Law"

The change in intensity of light (*dI)* after passing through a sample should be proportional to the following:

(a) path length, *b,* the longer the path, more photons should be absorbed

(b) concentration, *c*, of sample, more molecules absorbing means more photons absorbed

(c) intensity of the incident light *(I)*, more photons mean more opportunity for a molecule to see a photon

Thus,

dI is proportional to *bcI* or

$$\mathbf{dI/I = -k \times b \times c} \qquad \mathbf{(2.5)}$$

where *k* is a proportionality constant, the negative sign is shown because this is a decrease in intensity of the light, this makes *b*, *c* and *I* always positive.

Integration of the above equation leads to Beer-Lambert's Law:

$$-\ln I/I_0 = kbc \qquad \mathbf{(2.6)}$$

$$-\log I/I_0 = 2.303\ kbc \qquad \mathbf{(2.7)}$$

Substituting, $\epsilon = 2.303\ k$

$$A = -\log I/I_0 \qquad \mathbf{(2.8)}$$

$$A = \epsilon \times b \times c \qquad \mathbf{(2.9)}$$

'A' is defined as absorbance and it is found to be directly proportional to the path length, *b*, and the concentration of the sample, *c* and ϵ is extinction coefficient.

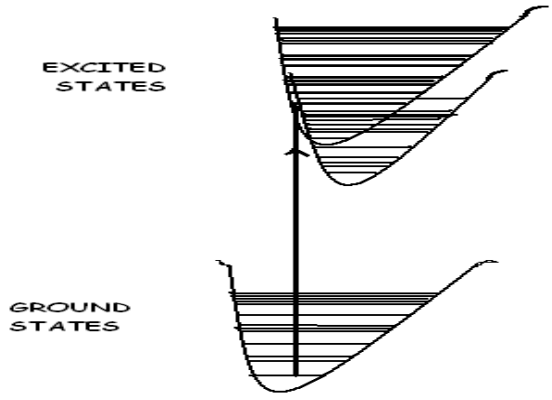

Figure 2.10: schematic of absorption process in a molecule**.**

The extinction coefficient is characteristic of the substance under study and of course, is a function of the wavelength. Molecules strongly absorb only in some regions of the electromagnetic spectrum. The photon carries a specific amount of energy defined by its wavelength (Recall Planck's equation: $E = hc/\lambda$). The molecule will only absorb a photon if the energy it carries matches a certain amount the molecule can use. In the ultraviolet-visible region, this energy corresponds to electronic excitations (promotion of electrons from occupied to unoccupied orbitals). The longest wavelength (the least energy) therefore corresponds to the energy difference between the ground and the first excited.

2.6.1.3 UV-Visible spectrometer

The basic parts of a spectrophotometer are a light source (often an incandescent bulb for the visible wavelengths, or a deuterium arc lamp in the ultraviolet), a holder for the sample, a diffraction grating or monochromator to separate the different wavelengths of light, and a detector. The detector is typically a photodiode or a CCD. Photodiodes are used with monochromators, which filter the light so that only light of a single wavelength reaches the detector. Diffraction gratings are used with CCDs, which collects light of different wavelengths on different pixels.

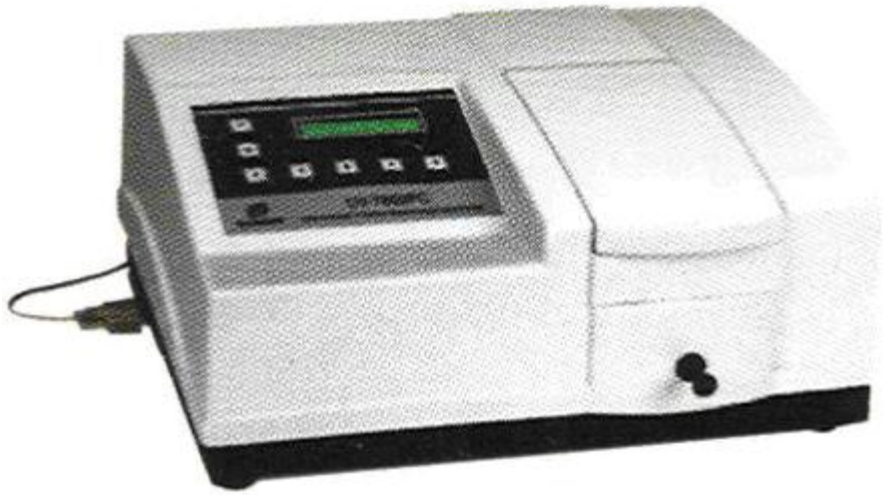

Figure 2.11: UV-Vis spectrophotometer.

The ultraviolet spectrum for a compound is obtained by exposing a sample of the compound to ultraviolet light from a light source, such as a Xenon lamp or deutrium lamp.The ultraviolet (UV) region scanned is normally from 200 to 400 nm, and the visible portion is from 400 to 800 nm. The detector records the ratio between reference and sample beam intensities (Io/I). The ratio I / I_o is called the *transmittance*, and is usually expressed as a percentage (%T). The absorbance, A, is based on the transmittance:

$$\boldsymbol{A = -\log(\%T)} \qquad \textbf{(2.10)}$$

At the wavelength where the sample absorbs a large amount of light, the detector receives a very weak sample beam. Once intensity data has been collected by the spectrometer, it is sent to the computer as a ratio of reference beam and sample beam intensities. The

computer determines at what wavelength the sample absorbed a large amount of ultraviolet light by scanning for the largest gap between the two beams.

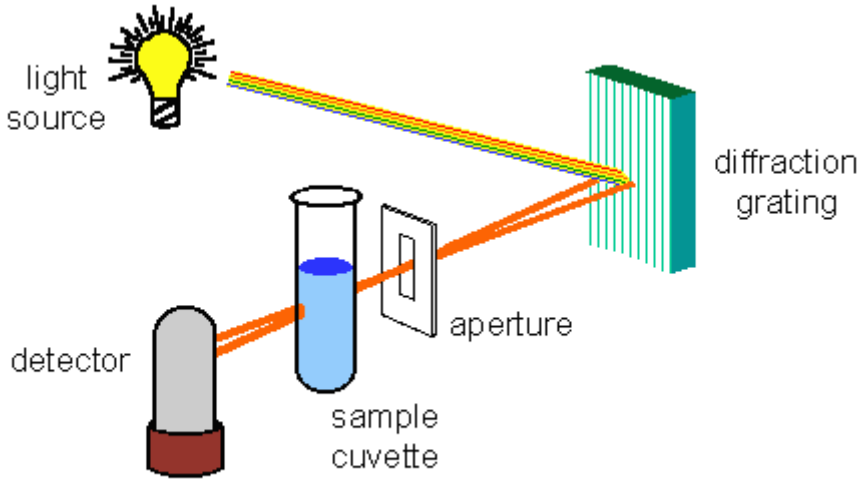

Figure 2.12: Schematic of internal view of transmittance measurement

When a large gap between intensities is found, where the sample beam intensity is significantly weaker than the reference beam, the computer plots this wavelength as having the highest ultraviolet light absorbance when it prepares the ultraviolet absorbance spectrum.

2.6.2 Photoluminescence

Photoluminescence spectroscopy is a contactless, nondestructive method of probing the electronic structure of materials. Light is directed onto a sample, where it is absorbed and imparts excess energy into the material in a process called photo-excitation. One way this excess energy can be dissipated by the sample is through the emission of light, or luminescence. In the case of photo-excitation, this luminescence is called photoluminescence. The intensity and spectral content of this photoluminescence is a direct measure of various important material properties.

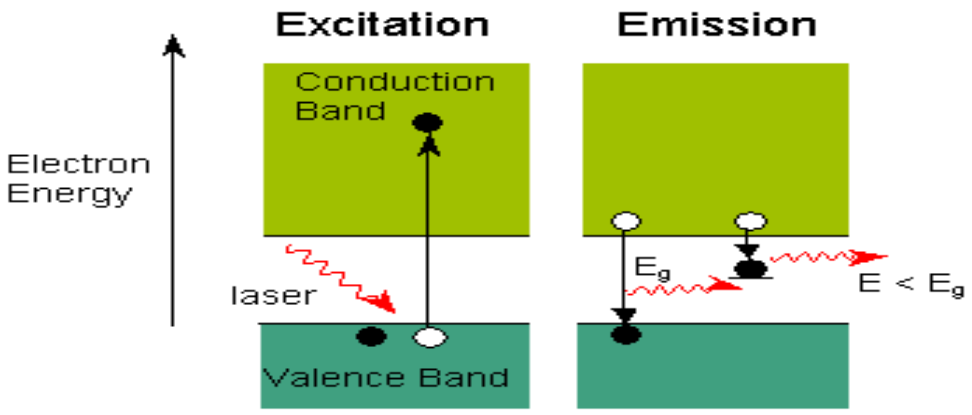

Figure 2.13: Energy level diagram to explain photoluminescence

In the above figure, E_g is the band gap energy. On the left a high energy laser photon dislodges an electron from its orbit. The electron loses energy until it reaches the bottom of the conduction band. The right hand diagram shows two possible transitions. On the left the electron combines immediately with a hole in the valence band emitting a photon of energy Eg. On the right it gets stuck in a 'mid-gap' state emitting a lower energy photon.

Photo-excitation causes electrons within the material to move into permissible excited states. When these electrons return to their equilibrium states, the excess energy is released and may include the emission of light (a radiative process) or may not (a nonradiative process).The energy of the emitted light (photoluminescence) relates to the difference in energy levels between the two electron states involved in the transition between the excited state and the equilibrium state. The quantity of the emitted light is related to the relative contribution of the radiative process.

2.6.2.1 Types of Photoluminescence:

1) Phosphorescence

2) Fluorescence

2.6.2.2 Phosphorescence

Phosphorescence is a process in which energy absorbed by a substance is released relatively slowly in the form of light. This is in some cases the mechanism used for "glow-in-the-dark" materials which are "charged" by exposure to light. Unlike the relatively swift reactions in a common fluorescent tube, phosphorescent materials used for these materials absorb the energy and "store" it for a longer time as the subatomic reactions required to re-emit the light occur less often.

Figure 2.14: phosphorescent material in day light, visible blue light and in dark

Phosphorescence is a specific type of photoluminescence related to fluorescence. Unlike fluorescence, a phosphorescent material does not immediately re-emit the radiation it absorbs. The slower time scales of the re-emission are associated with "forbidden" energy state transitions in quantum mechanics. As these transitions occur less often in certain materials, absorbed radiation may be re-emitted at a lower intensity for up to several hours.

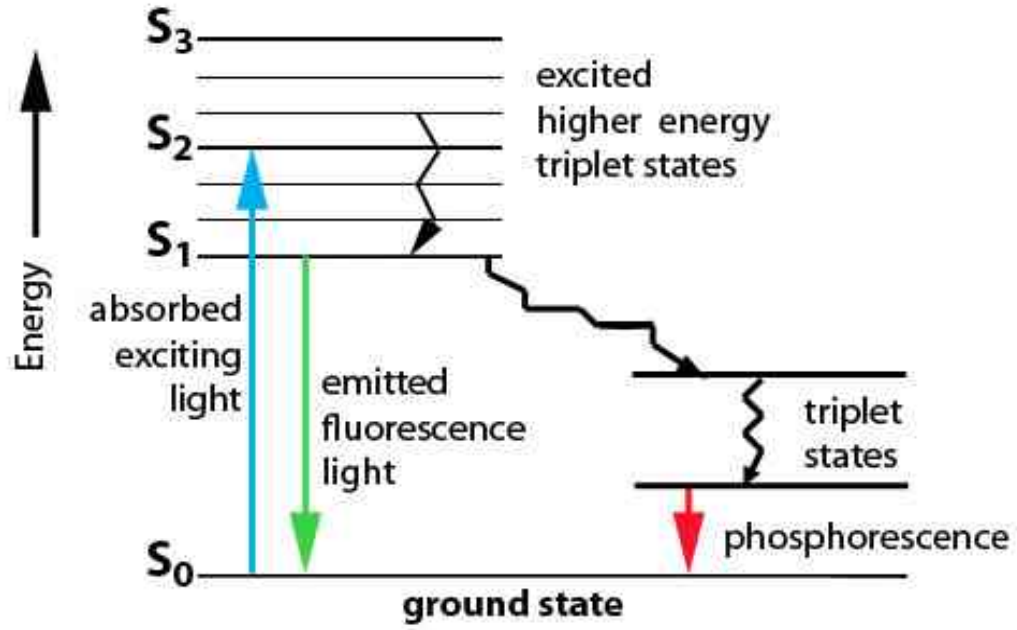

Figure 2.15: Phosphorescence and fluorescence processes

2.6.2.3 Fluorescence

Fluorescence is a luminescence that is mostly found as an optical phenomenon in cold bodies, in which the molecular absorption of a photon triggers the emission of with a longer (less energetic) wavelength. The energy difference between the absorbed and emitted photons ends up as molecular rotations, vibrations or heat. Sometimes the absorbed photon is in the ultraviolet range, and the emitted light is in the visible range, but this depends on the absorbance curve and Stokes shift of the particular fluorophore.

2.6.2.4 Information:

- Band Gap Determination

The most common radiative transition in semiconductors is between states in the conduction and valence bands, with the energy difference being known as the band gap. Band gap determination is particularly useful when working with new compound semiconductors.

- Impurity Levels and Defect Detection

Radiative transitions in semiconductors also involve localized defect levels. The photoluminescence energy associated with these levels can be used to identify specific defects, and the amount of photoluminescence can be used to determine their concentration.

- Recombination Mechanisms

The return to equilibrium, also known as "recombination," can involve both radiative and non-radiative processes. The amount of photoluminescence and its dependence on the level of photo-excitation and temperature are directly related to the dominant recombination process. Analysis of photoluminescence helps to understand the underlying physics of the recombination mechanism.

- Material Quality

In general, non-radiative processes are associated with localized defect levels, whose presence is detrimental to material quality and subsequent device performance. Thus, material quality can be measured by quantifying the amount of radiative recombination.

CHAPTER 3

METHODS OF PREPARATION & SYNTHESIS

3.1 EXPERIMENTAL

3.1.1 Method of Preparation

One-dimensional nanostructures have been called by a variety of names including: whiskers, fibres, nanowires and nanorods. Although whiskers and nanorods are in general considered to be shorter than fibres and nanowires, the definition is often a little arbitrary. In addition, one-

dimensional structures with diameters ranging from several nanometers to several hundred microns were referred to as whiskers and fibers in the early literature, whereas nanowires and nanorods with diameters within the range of 1-100 nm are used predominantly in the recent literature.

Many techniques have been developed in the synthesis and formation of one-dimensional nanostructured materials, though some techniques have been explored extensively, while others have attracted far less attention [56]. These techniques can be generally grouped into four categories:

(1) Spontaneous growth:
- Evaporation (or dissolution)- condensation
- Vapor (or solution)-liquid-solid(VLS or SLS) growth
- Stress induced recrystallization

(2) Template-based synthesis
- Electroplating and electrophoretic deposition
- Colloid dispersion, melt or solution filling
- Conversion with chemical reaction

(3) Electrospinning.

(4) Solvothermal.

(5) Lithography.

Spontaneous growth, template-based synthesis, electrospinning and solvothermal are considered as a bottom-up approach, whereas lithography is a top-down technique.

3.1.2 Solvothermal Technique

Solvothermal processes can be described as a reaction or a transformation of precursor(s) in presence of a solvent in a close system and at a temperature higher than the boiling temperature of the solvent. Solvothermal process is a powerful route for preparing non-oxide nanomaterials. This route is similar to the hydrothermal route where the synthesis is conducted in stainless steel autoclave with the only difference is that the precursor solution is non-aqueous [57]. With

solvothermal synthesis certain experimental parameters or conditions can easily alter the shape, type, size, size distribution, surface area and the crystallinity. Some of these experimental parameters may include reaction temperature, reaction time, solvent type, surfactant type, precursor type etc.

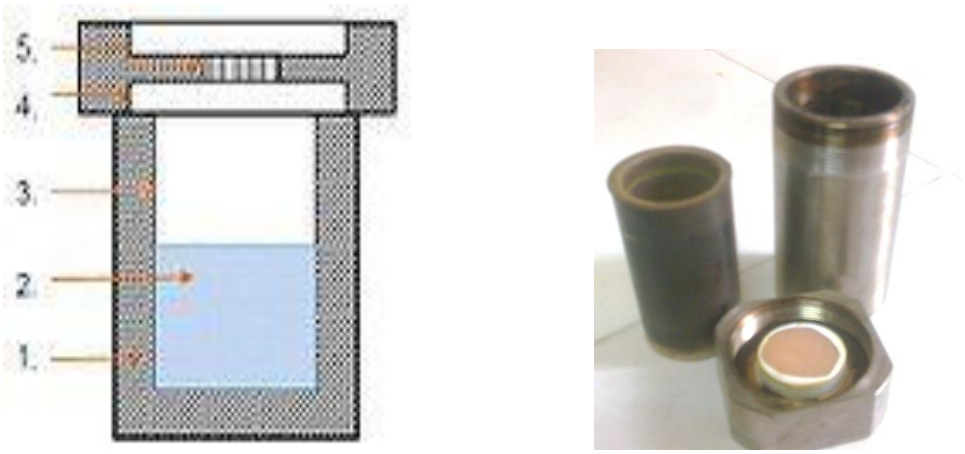

(a) (b)

Figure 3.1: **(a)** Schematic view of an autoclave (1) stainless steel autoclave (2) precursor solution (3) Teflon liner (4) stainless steel (5) steel lid (6) spring, **(b)** Photographic view of an autoclave

By using organic solvents under supercritical conditions as reaction media, chemical reaction and crystallization can be synchronously realized. Materials including diamond, carbon nanotubes, a series of carbides, nitrides, borides, phosphides, III-V and II-VI group semiconductor nanomaterials have been prepared via this method at conditions milder than those of traditional methods. As a low-temperature and convenient synthetic technique, solvothermal process is an exciting, promising approach for designing and preparing advanced materials.

Solvothermal processes can be described as the reaction or the decomposition of precursor(s) in presence of a solvent in a close system at a temperature higher than the solvent boiling point [58]. Consequently, pressure parameter is involved. Solvothermal reactions are governed by different factors:

- the nature of the precursors, in particular their physical and chemical properties (solubility, thermal stability)
- the nature of the solvent (solvatation, polarity, viscosity, ability to stabilize some complexes as intermediate steps).
- thermodynamical properties used during such a process (P and T)

Pressure and temperature can play an important role, some properties of the solvent such as density, viscosity changing drastically versus such parameters. Consequently the diffusion and reactivity of chemical species can be strongly affected. In a general way, solvothermal processes were developed in mild temperature conditions. Solvothermal processes concern either supercritical or subcritical conditions, homogeneous or heterogeneous systems, and thermodynamical parameters (P and T) play an important role. The main interest of solvothermal reactions is the improvement of the chemical reactivity, and in such a case the nature of the reagents and the physical-chemical properties of the solvent are important.

3.1.3 Role of the solvent in Solvothermal processes

Solvent plays a key role in solvothermal processes. Four examples can illustrate such a role:

(i) the orientation of the structural form

(ii) the development of a specific shape for nanocrystallites

(iii) the formation of specific metastable compounds through template action

(iv) the role of the oxidation – reduction properties.

3.2 Synthesis

In the present work, six samples of cadmium sulphide nanorods doped with terbium (with atomic concentrations of Tb: 0%, 0.1%, 0.5%, 1.0%, 3.0%, 5.0%)) were prepared by solvothermal technique in an autoclave cell.

The following chemicals have been used for the synthesis:

- Source of Cd ions, $Cd(ac)_2$
- Source of S ions, thiourea CH_4N_2S
- Source of the dopant Tb ions, terbium chloride $Tb(Cl)_3$
- Solvent, ethylenediamine (70% of the volume of cell)

Washing of the synthesized sample, to remove the by-products adhered to the surface of nanoforms, has been done by using double distilled water and ethyl alcohol. The molar ratio of the Cd salt to that of the sulphur source is 1:3.

Cadmium acetate (2.5653g), thiourea (2.2836g) and terbium chloride were completely dissolved in ethylene diamine (35 ml) solution in the autoclave. The mixture formed above was kept in an oven preheated to a temperature of 200^0C for 10 hours. The yellow precipitate formed in above process was filtered and washed several times with double distilled water and ethyl alcohol. The composite was then dried in an oven at 60^0C for one day. When the precipitates were completely dried, they were crushed to fine powder by grinding process and the nanorods so obtained were preserved in air tight appendrophs.

3.3 Heat treatment

Since heat treatment in air is known to cause oxidation of CdS, the as-synthesized nanorods were heated in nitrogen atmosphere at 200^0C for 2 hours.

Chapter 4

Results and Discussion

4.1. X-ray Diffraction (XRD) Studies

XRD studies are an efficient tool for analyzing the structural properties of the sample. In the present studies, XRD patterns have been recorded using X'PERT PRO Panalytical powder X-ray diffractometer using characteristics wavelength of 1.5418 *Å*. The powdered sample has been used as such for the XRD characterization, without any prior specimen preparation. The XRD pattern of synthesized and heat treated (200^{o} C for 2 hours in nitrogen gas atmosphere) samples of CdS doped with Terbium, 0.1% and 3.0%, are shown in the figures 4.1 and 4.2 respectively.

Tables 4.1 and 4.2 show the observed peak position, the miller indices and the intensity of the diffraction peaks for the CdS:Tb nanorods with Tb concentration 0.1% and 3.0 % respectively. Comparison of the recorded XRD pattern with standard JCPDS data file 41-1049 confirms the hexagonal wurtzite phase of the nanorods. Comparison of the standard and the observed intensities of the diffraction peaks, table 4.1 and 4.2, show that the peak intensity for (110) plane has increased, whereas there is a decrease in observed intensities for all other diffraction peaks. This shows higher order of orientation of the nanorods perpendicular to the (110) plane.

Moreover, the sharp peaks as shown in figures 4.1 and 4.2, show high degree of crystallanity in the synthesized nanorods. No impurity or dopant related peak has been observed in the XRD pattern.

2θ (Degree)	***(hkl)***	**Observed Intensity**	**Standard Intensity**
24.896	100	74	62
26.513	002	87	91
28.129	101	100	100
36.694	102	28	29
43.751	110	59	48
47.893	103	43	50

50.911	200	13	8
51.822	112	40	31
52.821	201	20	15
58.387	202	1	3

Table 4.1: Observed and standard data of the diffraction peaks for the CdS:Tb (0.1%) sample

2θ (Degree)	***(hkl)***	**Observed Intensity**	**Standard Intensity**
24.818	100	73	62
26.544	002	80	91
28.270	101	97	100
36.605	102	25	29
43.711	110	61	48
47.870	103	43	50
50.934	200	13	8
51.941	112	43	31
52.953	201	18	15
58.437	202	1	3

Table 4.2: Observed and standard data of the diffraction peaks for the CdS:Tb (3.0 %) sample

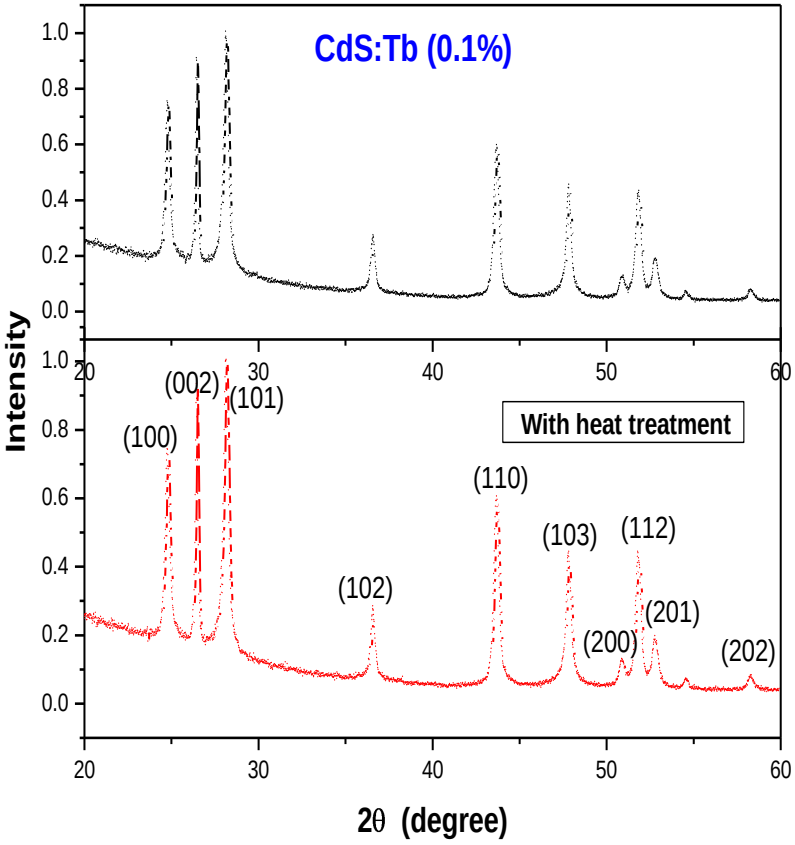

Figure 4.1: XRD pattern of synthesized and heat treated samples of CdS:Tb nanorods (0.1% Tb).

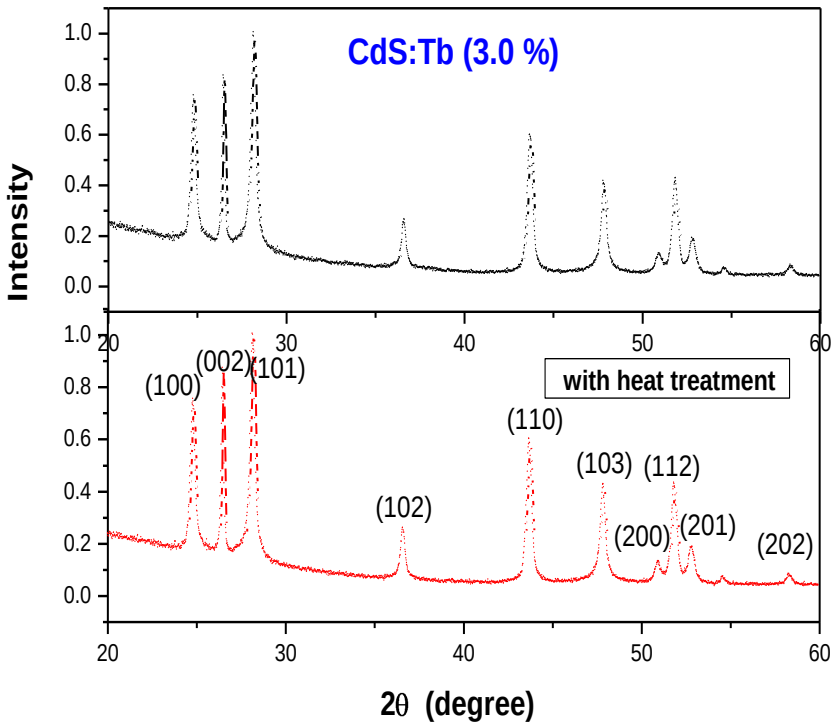

Figure 4.2: XRD pattern of synthesized and heat treated samples of CdS:Tb nanorods (3.0% Tb).

Average crystallite size of the nanostructures has been calculated from the recorded XRD pattern using well known Scherrer`s equation [56]:

$$D = 0.94\lambda / B \cos\theta \qquad (4.1)$$

where ***D*** is the average crystallite size, λ is the wavelength of incident X-rays, ***B*** is the full width at half maximum (FWHM) of diffraction peak (in radians) and θ is the position of the diffraction peak in the diffractogram. The mean calculated crystallite size in each case is ~ 55 nm.

It has been observed from the XRD pattern shown in figure 4.1 and 4.2, that there is no change in the crystal structure of the CdS:Tb nanorods on heat treatment of 200^{o} C for 2 hours in the

nitrogen gas atmosphere. The FWHM, peak positions and the intensities of the samples have not changed after the heat treatment showing the structural stability of the synthesized samples.

4.2. Energy Dispersive X-ray (EDAX) Spectroscopy

The composition of the CdS:Tb (1.0%) nanorods was analyzed by EDAX spectroscopy, using Noran System Six, as shown in figure 4.3. Electron beam induced inner-shell ionization and subsequent emission of characteristic fluorescence are analyzed in order to obtain the composition. As shown in figure 4.3, Cd L-fluorescence (Lα in the 3-4 keV energy range), S K-fluorescence (Kα in the 2.0-2.5 keV energy range) and Tb L & M-fluorescence (Lα, Lβ and Lγ in the energy range 6.0-8.5 keV, and Mα in the energy range 1-2 keV) are observed. This fluorescence spectrum shows the presence of Cd, S and Tb as the elementary components in the atomic percentage respectively, 48.55 %, 51.0 % and 0.45 %. This shows that Tb has replaced Cd upto only 0.45 atomic %, whereas 1.0 % concentration of Tb has been added during the synthesis process. The concentration of S is slightly more than that of Cd as expected. This is due to the fact that the molar ratio of Cd and S taken during the synthesis was 1:3. Quite an amount of S is also removed along with the byproducts of the reaction.

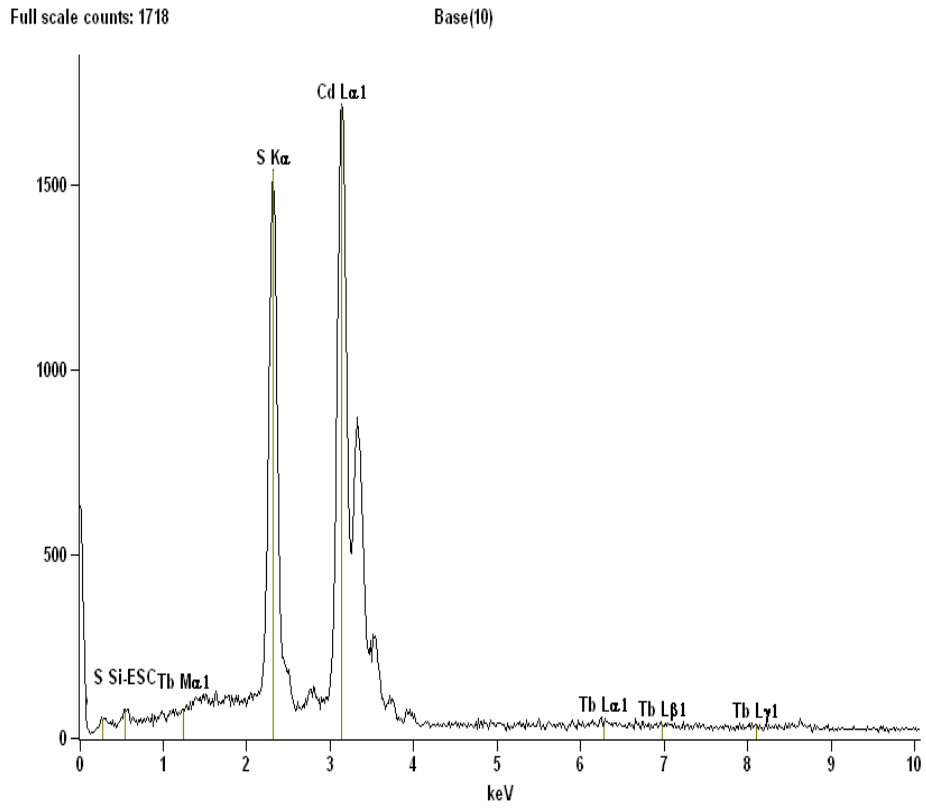

Figure 4.3: EDAX spectrum of the CdS:Tb (1.0 %) sample

4.3. Scanning Electron Microscopy (SEM)

Microstructures of the nanoforms were studied through scanning electron microscopy (SEM, FEI, Nova 200 NanoLab). The specimen preparation was done by sputtering a thin layer of gold on the samples placed on the SEM stubs, using a spin coater. This has been done to make the specimen conducting in nature. Figures 4.4, 4.5 and 4.6 show the SEM images of the undoped and Tb doped (1.0 at. % and 5.0 at. %) nanorods. As observed from figures 4.4 (a, b), the CdS nanorods have an average diameter of 60 nm, and the length is varying from 311 to 540 nm. On doping the CdS nanorods with Tb (1.0 %), the average diameter of the nanorods has increased to 72 nm and the length is varying between 414 to 903 nm, as shown in figures 4.5 (a, b). With further increase in the dopant concentration to 5.0 %, the average diameter of the nanorods has increased to 92 nm and the length is lying between 910 nm to 1006 nm.

This shows that the morphology of the nanorods is highly influenced by the presence of Tb ions as a dopant, and it is changing with increase in the concentration of Tb. The synthesized nanorods are of uniform diameter throughout the length of the nanorods, giving them a cylindrical shape. The yield of the nanorods is quite high. This shows the effectiveness of the solvothermal technique used to synthesize the sample.

Moreover on comparing the SEM images in CdS:Tb nanorods having Tb concentration of 0 %, 1.0 % and 5.0 %, it seems that the roughness of the surface of the nanorods is increasing. But to further confirm this result, a detailed insight of the surface is required. This can be achieved through Transmission Electron Microscopy (TEM) and Atomic Force Microscopy (AFM).

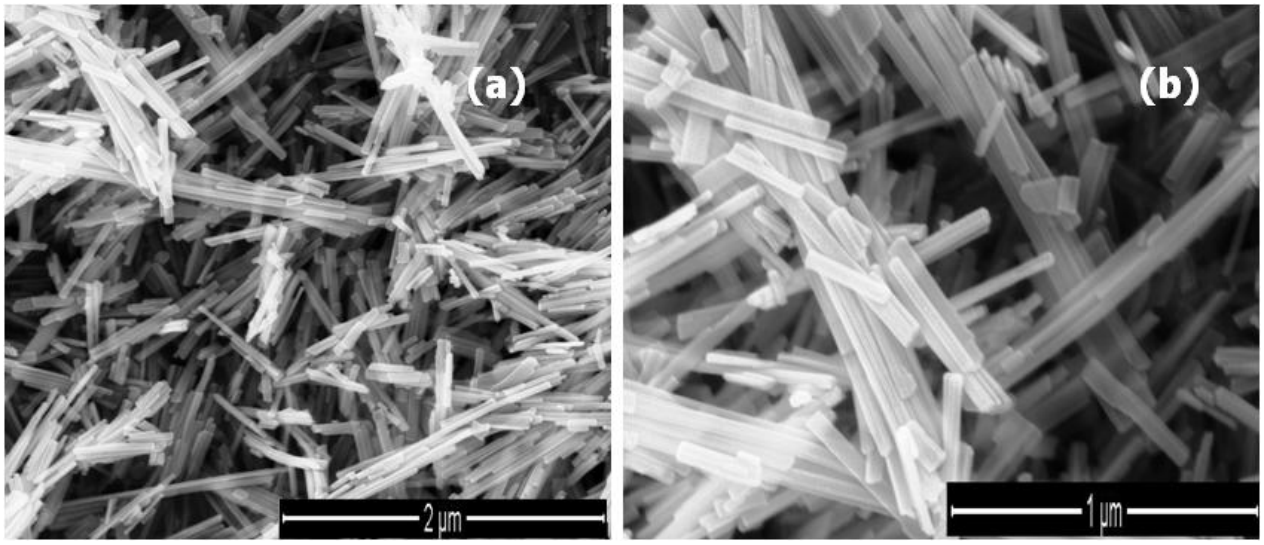

Figure 4.4: (a) SEM images of CdS (undoped) nanorods, **(b)** image at higher magnification

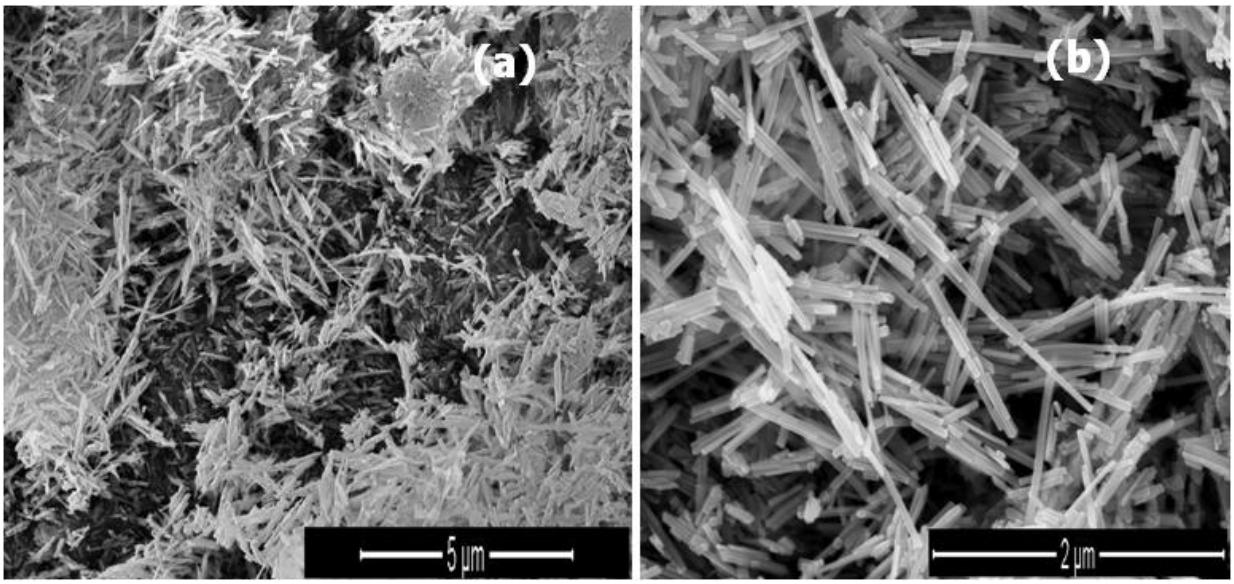

Figure 4.5: (a) SEM images of CdS:Tb (1.0%) nanorods, **(b)** image at higher magnification

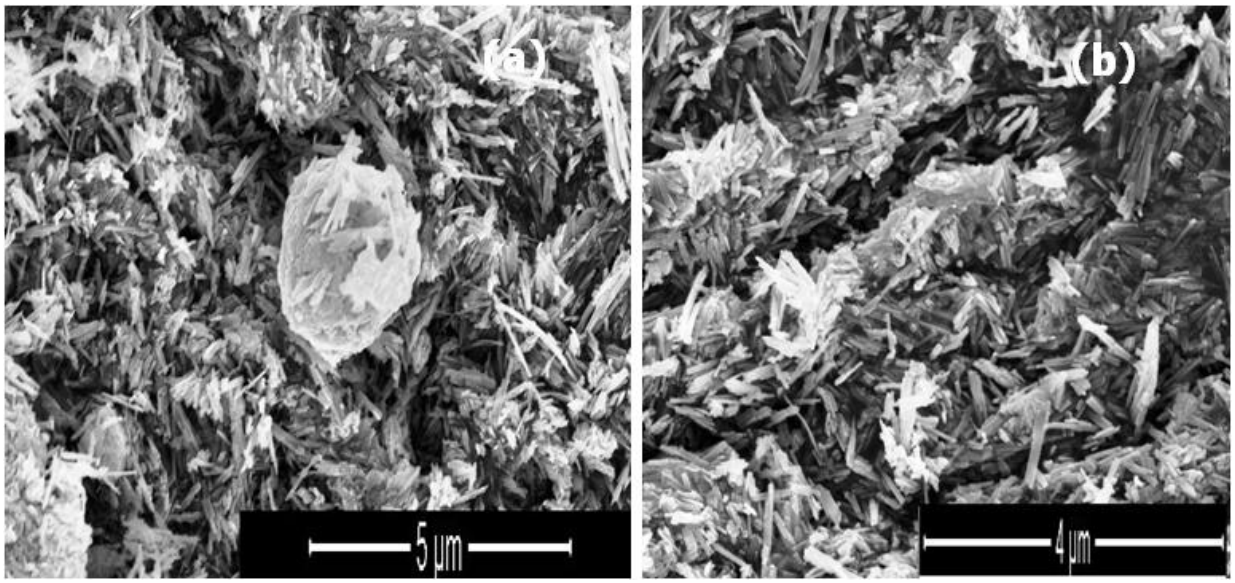

Figure 4.6: (a) SEM images of CdS:Tb (5.0%) nanorods, **(b)** image at higher magnification

4.4. Fourier Transform Infrared (FTIR) Spectroscopy

FTIR spectroscopy has been used to investigate the organic chemical components present on the surface of the synthesized samples. Powered samples have been used with FTIR Spectrum BX-II (Perkin Elmer) spectrometer, without any further specimen preparation.

As shown in the figures 4.7, 4.8 and 4.9, the weak peak appearing at 662 cm^{-1} indicates the presence of C-S linkage in the CdS nanorods (for as-synthesized and heat treated samples).The weak peaks observed at 1228 cm^{-1} can be attributed to the presence of C(=O)-O stretching vibrations in acetates or can also be due to C-H bending vibration. In case of the heat treated samples, this peak has become broader.

The FTIR peak at 1228 cm^{-1} might be due to the unconjugated C-N linkage in primary, secondary, and tertiary amines. The intensity of this peak is seen to be decreased after the heat treatment of the sample. This shows that the C-H and C-N bonding are becoming more weak on heat treatment The C=C stretching mode of unconjugated alkenes shows a moderate to weak absorption at 1664 cm^{-1} or this peak might be a resultant of N-H bending or stretching vibrations. The weak peak positioned at 2116 cm^{-1} is due to C≡C triple bond. The broad band at 3245 cm^{-1} is a consequence of O-H, N-H stretching vibrations and this broad band appears to get broaden with heat treatment as well as with increase in the concentration of Tb in the CdS nanorods.

These results support the presence of ethylenediamine complexes with Cd ions on the surface of the nanorods, which show a smoothening effect on heating the CdS:Tb nanorods at a temperature of 200^{o} C for 2 hours in nitrogen gas atmosphere.

A strong peak at 2363 cm^{-1}, which is generally attributed to the presence of CO_2 in the sample, is actually a reference/sample holder`s peak coming from the FTIR spectrometer in case of all the samples.

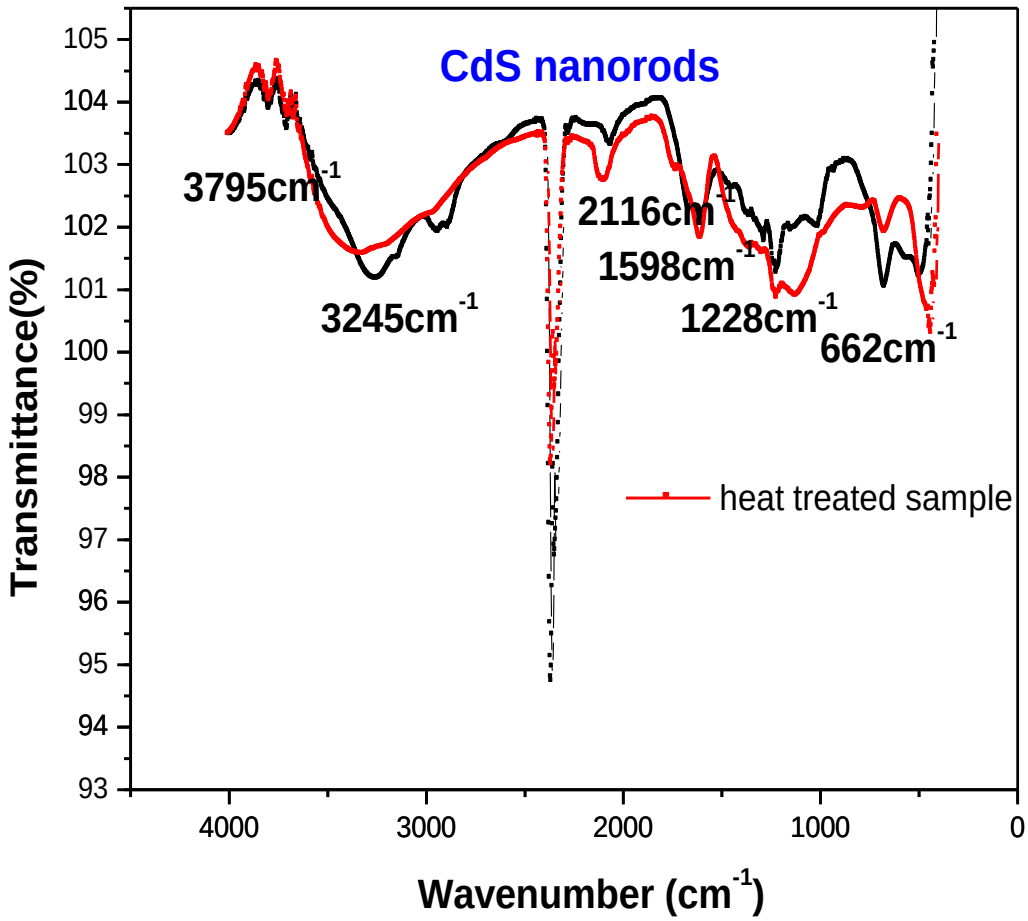

Figure 4.7: FTIR spectra of CdS nanorods showing the effect of heat treatment

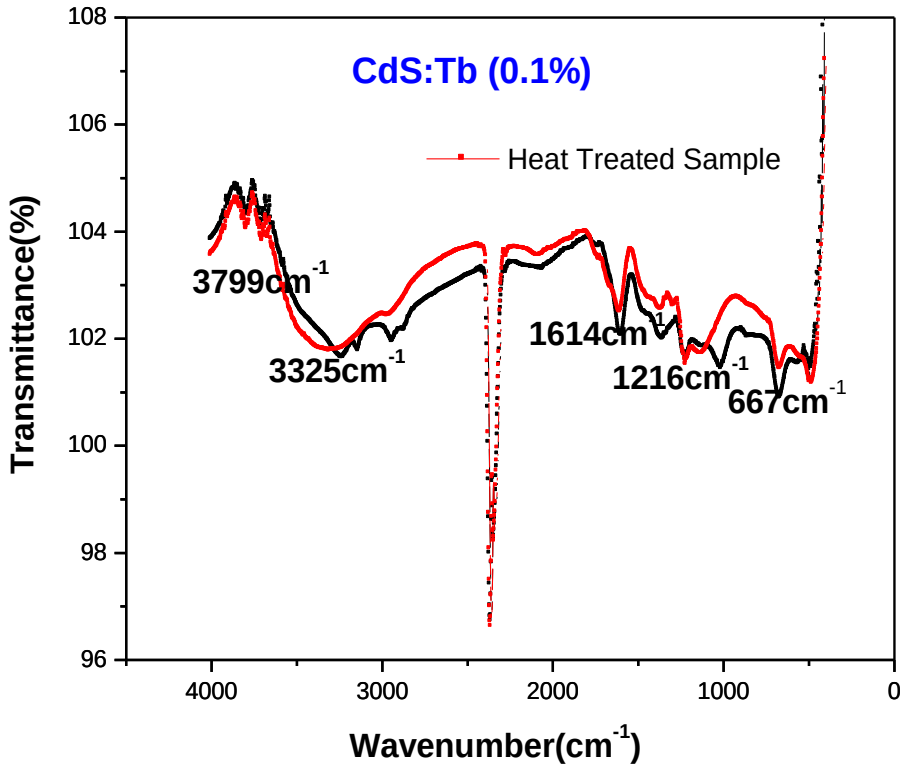

Figure 4.8: FTIR spectra of CdS nanorods doped with Tb (0.1%) and the effect of heat treatment

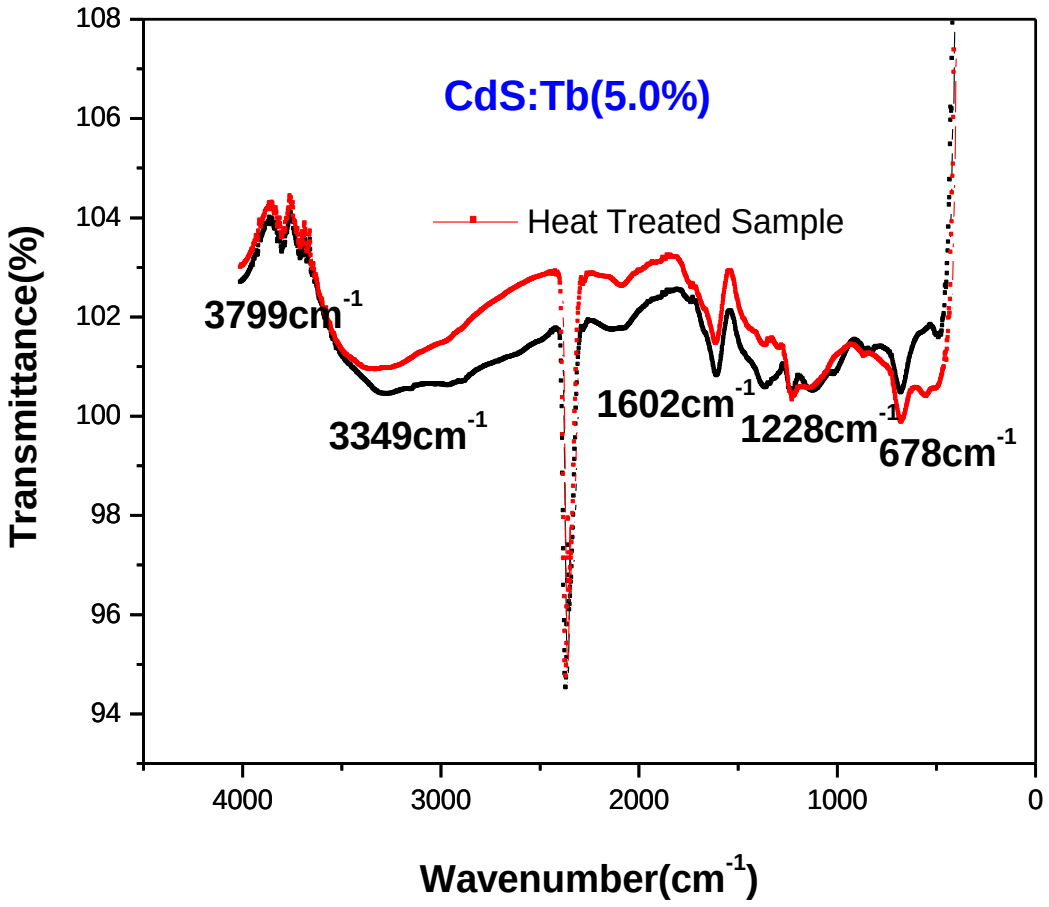

Figure 4.9: FTIR spectra of CdS:Tb (5 %) with the effect of heat treatment

4.5. OPTICAL CHARACTERIZATION

4.5.1 UV-Visible Absorption Studies

Undoped and Tb doped CdS nanorods, finely dispersed in ethanol, have been used for the UV-visible absorption studies by using Specord 205 spectrophotometer (Analytik Jena). As shown in figure 4.10, the absorption spectra of CdS nanorods doped with 1.0 % Tb shows a distinguished excitonic peak at around 491 nm, which has been red shifted by 10 nm, on heat treatment of the sample at 200^{o} C for 2 hours in nitrogen gas atmosphere.

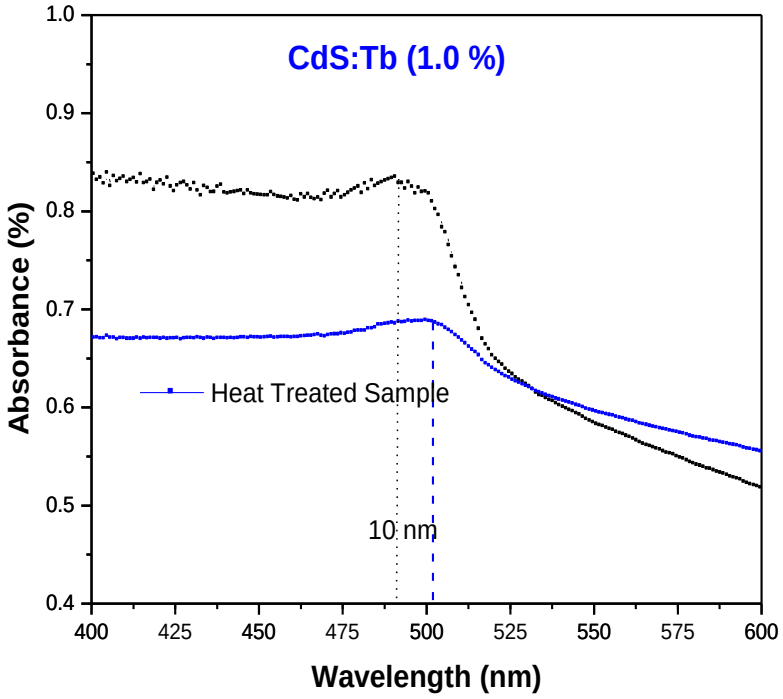

Figure 4.10: Absorption spectra of CdS doped with terbium (1%), synthesized and heat treated

CdS is a direct band gap semiconductor, E_g = 2.42 eV. Using the Tauc`s relation to calculate the band gap of the nanomaterials, $(\alpha h\upsilon)^2$ has been plotted against the energy values in eV. Where α, is the absorption coefficient; h, is the Planck's constant; and υ is the frequency of the light waves. On extrapolating the straight portion of the curve so obtained, we can estimate the band gap value of the nanomaterials. However, the minima obtained from the first derivation of the absorption spectra, also helps in the estimation of the band gap value.

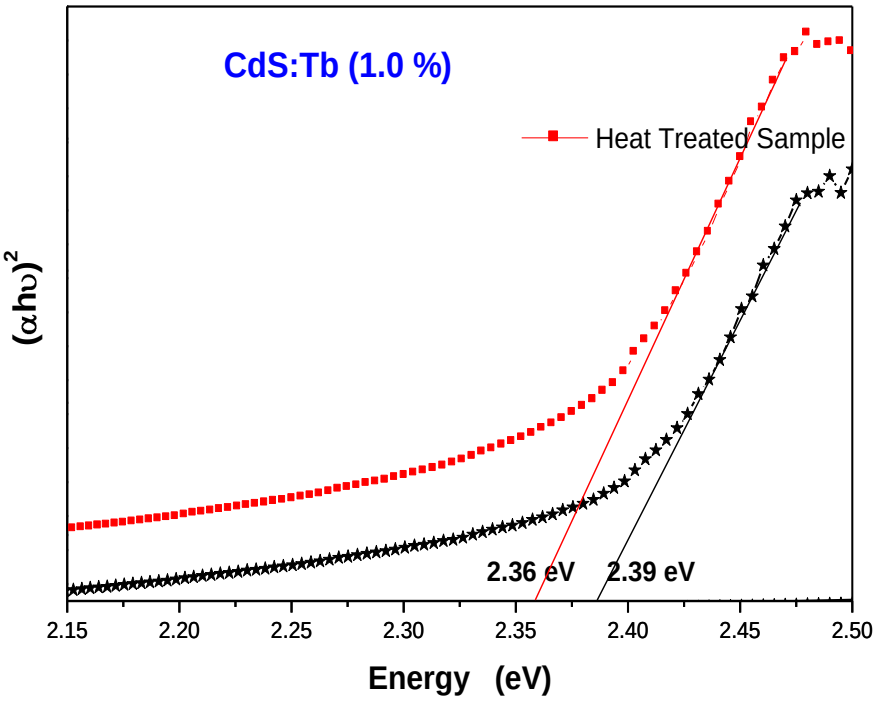

Figure 4.11: $(\alpha h\upsilon)^2$ vs hυ plot of synthesized and heat treated CdS nanorods doped with terbium (1%)

As shown in figure 4.11, the band gap value of Cds:Tb (1%) nanorods is 2.39 eV, which is lesser as compared to the bulk value of 2.42 eV. This may be due to the large number of surface

defects owing to higher surface to volume ratio in case of nanoforms. Moreover, further red shift of 0.03 eV has been observed in case of heat treated samples. This may be attributed to a small increase in the size of the nanorods on heat treatment, due to nucleation process.

4.5.2 Photoluminescence (PL) Studies

Room temperature PL spectra of the finely dispersed CdS:Tb nanorods have been measured using a xenon lamp source spectrophotometer (Cary Varian), at an excitation wavelength of 325 nm. As shown in figure 4.12, the emission at 525 nm is due to the near band edge transition of CdS. This can also be correlated from the absorption spectra having the band gap value of nearly 518 nm. However, the emission at 543 and 573 nm can be attributed to the surface related/trap defects, due to the presence of sulfur or cadmium vacancy or interstitial. Blue colored high level transitions have been observed at 424 and 442 nm. The intensity of these emissions has increased with increase in Tb concentration as shown in figure 4.12. Moreover, a Tb ion related emission has been observed at 485 nm.

As shown in figure 4.13, an additional emission has been observed in heat treated CdS samples at 363 nm. This UV region emission has further broadened in case of Tb doping of 1.0 %, and the peak position has shifted to around 386 nm. This peak has been observed to broaden further and shift to 393 nm, on increase in Tb concentration, as shown in figures 4.14, 4.15 and 4.16. This may be due to some radiative high level transitions arising due to heat treatment. Further studies are required to probe into these changes in the emission spectra.

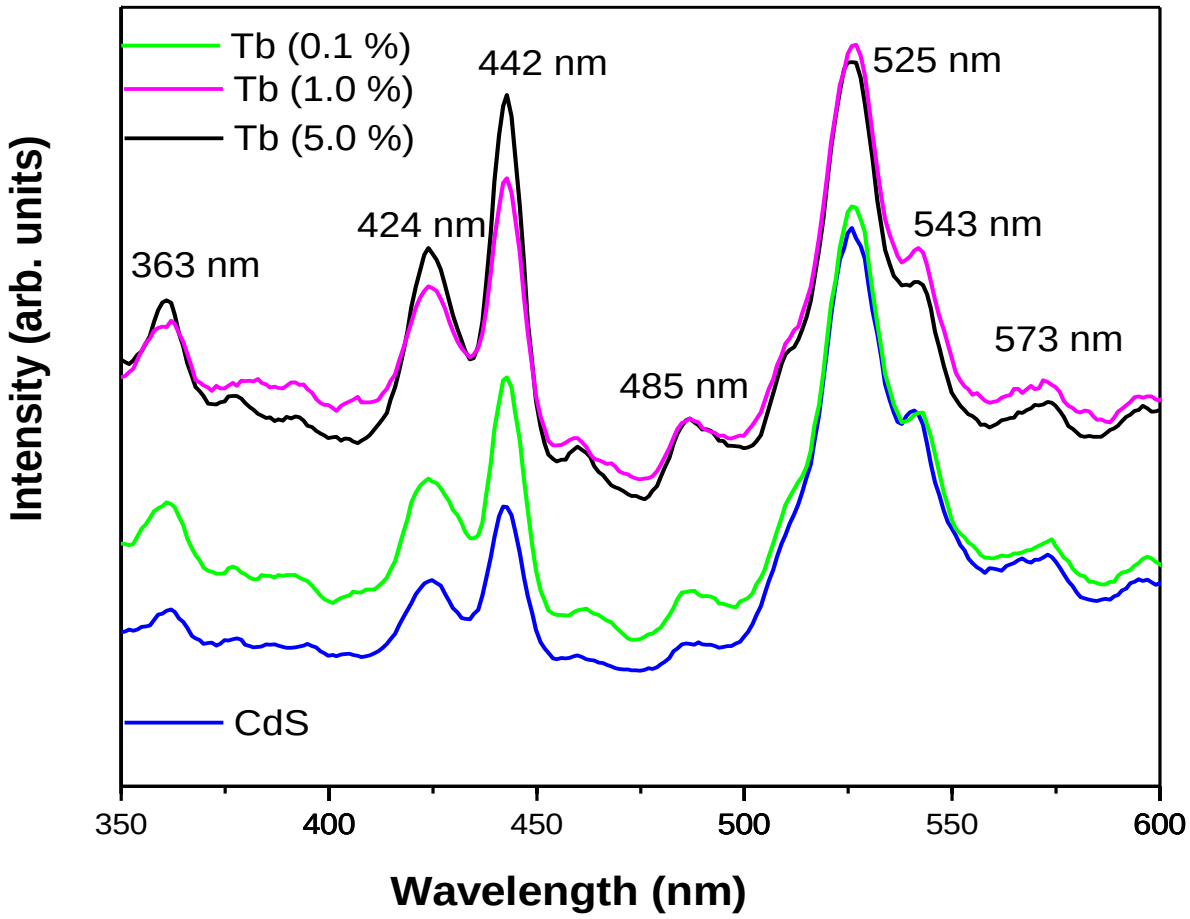

Figure 4.12: PL spectra of the undoped and Tb doped CdS nanorods at 325 nm excitation wavelength

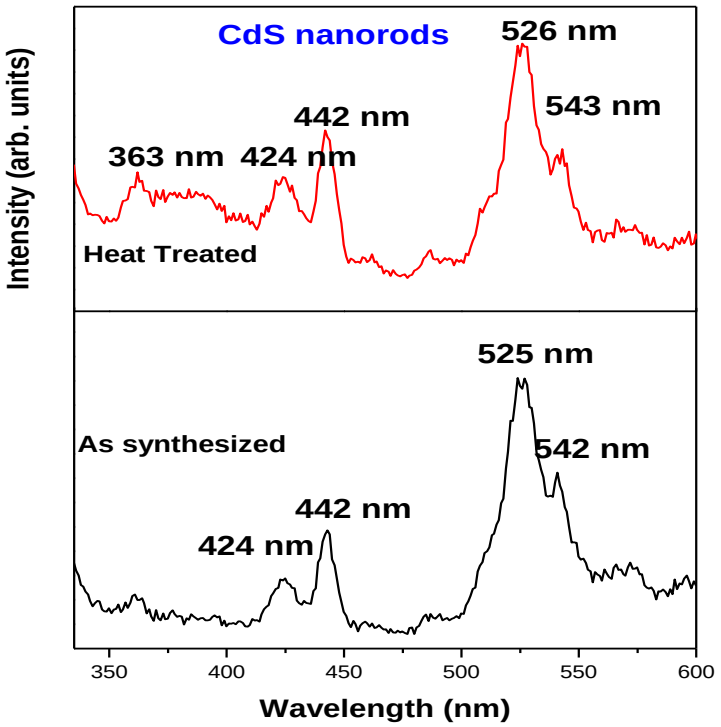

Figure 4.13: Room temperature PL spectra of CdS nanorods with and without heat treatment using the excitation wavelength of 325 nm

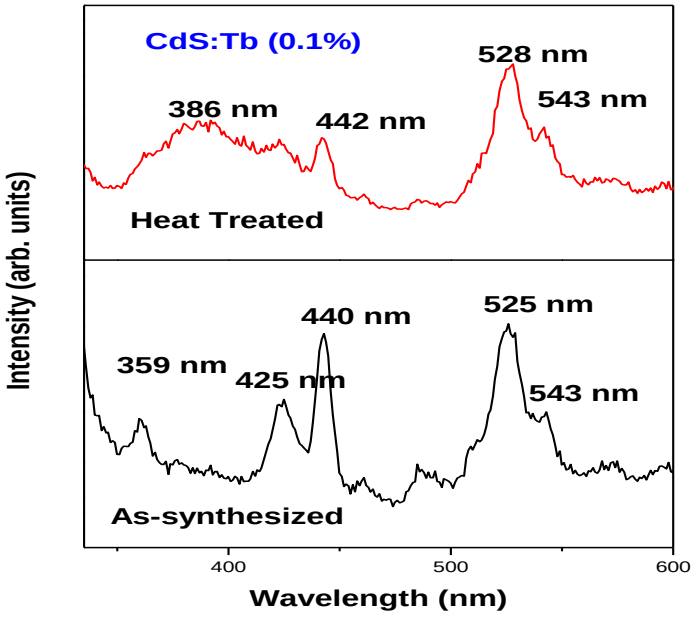

Figure 4.14: Room temperature PL spectra of CdS:Tb (0.1%) nanorods with and without heat treatment using the excitation wavelength of 325 nm.

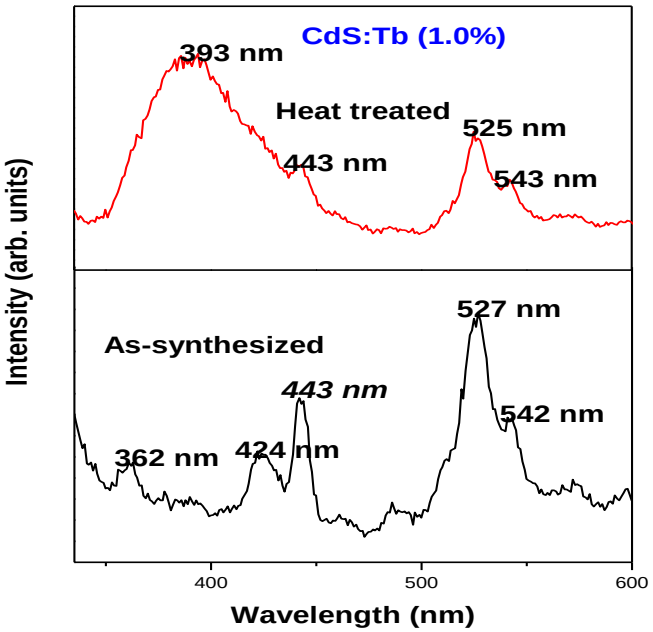

Figure 4.15: Room temperature PL spectra of CdS nanorods with and without heat treatment using the excitation wavelength of 325 nm

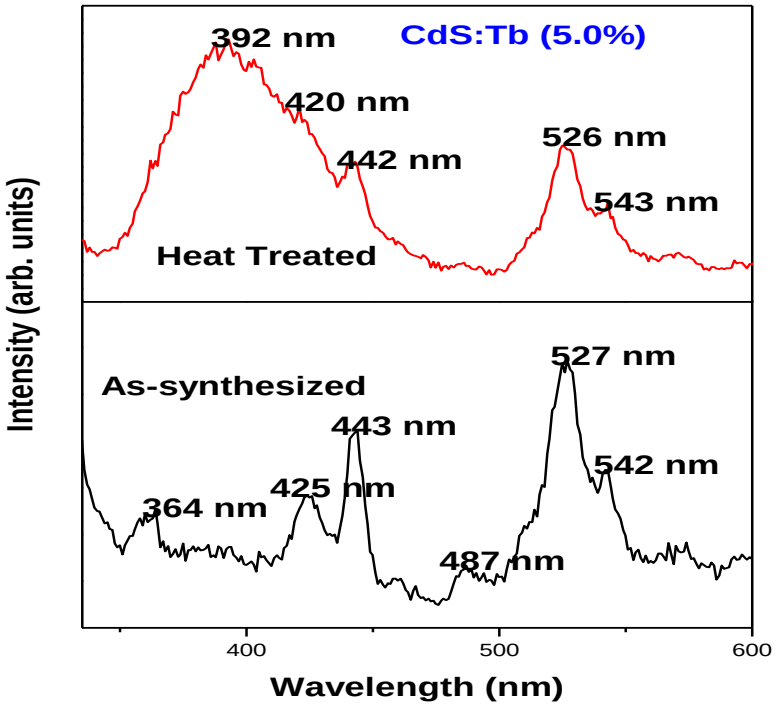

Figure 4.16: Room temperature PL spectra of CdS:Tb (5.0%) nanorods with and without heat treatment using the excitation wavelength of 325 nm

Chapter 5

Conclusions

Conclusions

The aim of the present work was to investigate the effect of doping and heat treatment on the structural and optical properties of CdS:Tb nanorods. The synthesis of these nanorods has been carried out by Solvothermal technique with ethylenediamine as the solvent, at 200^{o} C for 10 hours. The heat treatment to the samples has been given in nitrogen gas atmosphere at 200^{o} C for 2 hours. The work has been concluded as follows:

- Nanorods are found to have hexagonal structure with high degree of orientation along (100) plane.
- No structural changes have been observed in the XRD pattern of the nanorods on doping with Tb and after the heat treatment.
- The elemental analysis carried out by EDAX shows the expected percentage of elements of the sample i.e. Cd (48.55%), S(51%), Tb(0.45%).
- As observed from SEM, the diameter and length of the nanorods are found to increase with increase in the doping concentration. Moreover, the smooth and uniform surface of nanorods also becomes rough.
- FTIR studies revealed the presence of ethylenediamine complexes with Cd ions on the surface of the nanorods, which show a smoothening effect on heating the CdS:Tb nanorods.
- The absorption spectra of CdS nanorods doped with 1.0 % Tb shows a distinguished excitonic peak at around 491 nm, which has been red shifted by 10 nm, on heat treatment.
- The band gap of CdS:Tb nanorods, synthesized and heat treated, were calculated to be 2.39 eV and 2.36 eV respectively. This red shift has been attributed to a small increase in the size of the nanorods on heat treatment, due to nucleation process.
- The near band edge emission of CdS at 525 nm has been observed.
- The emissions at 543 and 573 nm can be attributed to the surface related/trap defects, due to the presence of sulfur or cadmium vacancy or interstitial. Blue colored high level transitions have been observed at 424 and 442 nm. The intensity of these emissions has increased with increase in Tb concentration. Moreover, a Tb ion related emission has been observed at 485 nm.

- An additional emission has been observed in heat treated CdS samples at 363 nm. This UV region emission has further broadened and red shifted with increase in Tb concentration. This may be due to some radiative high level transitions arising due to heat treatment.
- Further studies are required to probe into these changes in the emission spectra.

REFERENCES

[1] N. Lane, Journal of Nanoparticle Research 3 (2001) 95

[2] R. F. Service, Science 290 (2000) 1526.

[3] R. Spohr, "Ion tracks and microtechnology". Vieweg Verlagsgesellschaft, Braunschweig, 1990.

[4] M. Datta and D. Landolt, Electrochimica Acta 45 (2000) 2535.

[5] R. E. Howard, P. F. Liao, W. J. Skocpol, L. D. Jackel and H. G. Craighead, Science 221 (1983) 117.

[6] R. W. Keyes, IBM Journal of Research and Development, 44 (2000) 84.

[7] C. Tannoudji, B. Diu and F. Laloe, Quantum mechanics; 1st edn.; John Wiley & Sons: New York, 1997.

[8] C. Nutzenadel, A. Zuttel, D. Chartouni, G. Schmid, and L. Schlapbach, European Physical Journal D8 (2000), 245.

[9] A. N. Goldstein, C. M. Echer, and A. P. Alivisatos, Science 256 (1992) 1425.

[10] A. I. Ekimov and A. A. Onushchenko, Soviet Physics – Semiconductors 16 (1982) 775.

[11] R. Rossetti, S. Nakahara, and L. E. Brus, Journal of Chemical Physics 79 (1983), 1086.

[12] W. R. Datars and J. M. Mativetsky, Physica, B (2002) 191.

[13] R. M. Nyffenegger and R. M. Penner, Chemical Reviews 97 (1997) 1195.

[14] S. H. Sun, C. B. Murray, D. Weller, L. Folks and A. Moser, Science 28**7** (2000) 1989

[15] F. Sharifi, A. V. Herzog and R. C. Dynes, Physical Review Letters 71 (1993) 428.

[16] B. Das, S. Subramanium, and M. R. Melloch, Semiconductor Science and Techology 8 (1993) 1347.

[17] C. Vieu, F. Carcenac, A. Pepin, Y. Chen, M. Mejias, L. Lebib, L. Manin Ferlazzo, L. Couraud, and H. Launois, Applied Surface Science 164 (2000) 111.

[18] K. Zamani, Proceedings of Spie 4608 (2002) 266.

[19] A. Vilan and D. Cahen, Trends in biotechnology 20 (2002) 22.

[20] R. F. Service, Science 293 (2001) 782.

[21] G. Mahler, V. May, and M. Schreiber, Molecular electronics: properties, Dynamics, and Applications, Marcel Dekker, New York (1996).

[22] W. J. Lehmann, Luminescence 5 (1972) 87.

[23] J Zhang, F. Jiang and L. Zhang, Journal of Physical Chemistry, B108 (2004) 7002.

[24] P. Psuja, D. Hreniak and W. Strek, Journal of Nanomaterials, Article ID (2007) 81350.

[25] J. H. Zeng, T. Xie, Z. H. Li and Y. Li, Growth and design, 12 (2007) 2774.

[26] T. Carmen, R. K. Mehra, R. Kho, M. Kumke, Journal of Chemical Physics letters 377 (2003) 131

[27] C. Tiseanu, R. K. Mehra, R. Kho and M. Kumke, Journal of Physical Chemistry B107 (2003) 12153.

[28] P. V. Jyothy, K. A. Amrutha, J. Gijo and N. V. Unnikrishnan, Journal of Fluorescence 19 (2009) 165.

[29] N. J Hua, H. R. Nian, L. W. Lian, L. M. Tao and Y. T. Zhi, Journal of Physics 39 (2006) 2357.

[30] N. S. Gajbhiye, R. S. Ningthoujamn, A. Ahmad, D. K.Panda, S. S. Umare and S. J. Sharma Pramana Journal of Physics 70 (2008) 313.

[31] B. Julian, J. Planelles, E. Cordoncillo, P. Escribano, P. Aschehoug,C. Sanchez, B. Viana And F. Pelle , Journal of Materials Chemistry 16 (2006) 4612.

[32] V. Sivasubramanian, A. K. Arora, M. Premila, C. S. Sundar and V. S. Sastry, Physica E31 (2006) 93

[33] R. J Bandaranayke, G. W. Wen, J. Y. Lin, H. X. Jiang, C. M. Sorensen, Applied Physics Letters 67 (1995) 81.

[34] O. Z. Angel, A. E. E. Garcia, C. Falcony, R. L. Morales, R. R. Bon, Solid State Communications 94 (1995) 81.

[35] W. Wang, I. germanenko, M. S. El-Shall, Chemistry of Materials 14 (2002) 3028.

[36] C. B. Murray, D. J. Norris, M. G. Bawendi, Journal of American Chemical Society 115 (1993) 8076.

[37] R. J. Traill, R. W. Boyle, American Mineralogist 40 (1955) 555.

[38] Charles Kittel Introduction to Solid State Physics- 7th Edition (1995) Wiley-India ISBN 1081-265-1045-5

[39] Greenwood, N. Norman and A. Earnshaw (1997), *Chemistry of the Elements* (2nd ed.), Oxford: Butterworth-Heinemann, ISBN 0-7506-3365-4

[40] A. Luque and S. Hegedus, (2003), Handbook of Photovoltaic Science and Engineering John Wiley and Sons ISBN 0471491969

[41] D. C. Reynolds, G. Leies, L. L. Antes, R. E. Marburger, Physical Review 96(1954) 533.

[42] J. S. Meth et al., Aplied Physics Letters 444 (2003) 227

[43] J. S. Meth et al., Applied physics letters 84 (2004) 2922.

[44] C. Fouassier,(1994), *Luminescence* in Encyclopedia of Inorganic Chemistry, John Wiley & Sons ISBN 0471936200**.**

[45] A. K. Cheetham, P. Day (1992), Solid State Chemistry: Compounds Oxford University Press ISBN 0198551665

[46] W. J. Minkus, Physics Review 138 (1965) A1277.

[47] R. W. Smith, Physics Review 105 (1957) 900.

[48] Y. A. Akimov, A. A. Burov, Y. A. Drozhbin, V. A. Kovalenko, S. E. Kozlov, I. V. Kryukova, G. V. Rodichenko, B. M. Stepanov and V. A. Yakovlev, Soviet Journal of Quantum Electronics 2 (1972) 284.

[49] R. Agarwal, C. J. Barrelet, C. M. Lieber, Nano Letters 5 (2005) 917.

[50] Nanosized semiconductor particles in glasses prepared by the sol–gel method: their optical and potential uses, Journal of Alloys and Compounds, 341 (2002) 61.

[51] http://www.elementsales.com/re_exp/index.htm

[52] C. R. Hammond, "The Elements", in Handbook of Chemistry and Physics 81th edition

[53] H. B. Lei, Q. Q. Yang, J. L. Zhu, J. H. Gao, H. J. Wang and Q. M. Wang, Chinese Physics Letters 15 (1998) 72.

[54] K. Swiatek, M. Godlewski and D. Hommel, Physics Review B42 (1990) 3628.

[55] K. Swiatek, M. Godlewski, L. Niinisto and M. Leskela, Acta Physica Polonica A82 (1992) 769.

[56] G. Cao, "Nanostructures and Nanomaterials – Synthesis and Properties.", Imperial College Press (2004) 110-111.

[57] http://en.wikipedia.org/wiki/Solvothermal_Synthesis_of_titanium_dioxide.

[58] Z. Guifu, L. Hui, Z. Yuanguang, X. Kan and Q. Yitai , Nanotechnology 17 (2006) S313.